ASCE

Improved Design Shear Method for the Bolted Cold-Formed Steel Clip-Angle Connector

Nagaraju Mallepogu, S.M.ASCE[1]; and Mahendrakumar Madhavan, Ph.D., P.E., F.ASCE[2]

Abstract: In this paper, the ultimate shear capacity of the 3-bolt cold-formed steel clip-angle between the cold-formed steel (CFS) beam and column is evaluated through 54 laboratory tests. A series of experiments were conducted by varying (1) thickness, and (2) aspect ratio (L/D) of clip-angles for different depths (D) and widths (A). The experimental program consists of three phases of tests: (1) Phase-I: direct shear load tests on clip-angle attached to a CFS column through 4.6-grade bolts; (2) Phase-II: CFS column replaced with a hot-rolled steel (HRS) column, since the CFS column experienced bearing failure in Phase-I; and (3) Phase-III: 10.9-grade bolts used instead of 4.6, as the 4.6-grade bolts subjected to bolt shear failure in Phase-II. Failure modes observed in the test specimens are (1) shear local buckling of clip-angle; (2) column bearing failure; (3) bolt shear failure; and (4) tear failure in clip-angle. Design shear equations from the literature, for the bolted clip-angle, were found to be inefficient for the high-grade steel ($f_y = 375$ MPa to 550 MPa), and conservative for the commonly available low-grade steel ($f_y = 275$ MPa). Hence a new shear strength equation is suggested for the clip-angle from the collated data of the present study and past research work. A comparative study between 2-bolt and 3-bolt clip-angle configurations was conducted to evaluate the increase in shear strength. Reliability studies were conducted, and corresponding resistance and safety factors were suggested for the design shear strength calculation corresponding to load and resistance factor design (LRFD), limit state design (LSD), and allowable strength design (ASD) methods. **DOI: 10.1061/JSENDH.STENG-11666.** © *2023 American Society of Civil Engineers.*

Author keywords: Bolted clip-angle; Cold-formed steel beam-to-column connection; Column bearing failure; Reliability analysis.

Introduction

In the last decades, the use of cold-formed steel (CFS) sections has become more popular in lightweight commercial structures and industrial building constructions. CFS is preferred to hot-rolled steel (HRS) in steel construction where quality, as well as appearance, plays a vital role due to close dimensional tolerance and smooth surface finish. In addition, CFS sections are typically pre-galvanized, eliminating the need to paint the structure after fabrication. There are numerous advantages associated with CFS sections; some of them are its light weight, ease in handling and assembly, high strength to weight ratio, high dimensional precision, and better surface quality. Moreover, transportation is more cost-effective and easier due to the highly customized shapes of CFS members.

CFS members are often connected by an L-shaped connector known as a clip-angle. The thin-walled behavior of the clip-angle makes its failure modes complicated and requires that more attention be paid to its design. Being the weakest link in the CFS framing system, the clip-angles are vulnerable to premature failure. A typical application of a clip-angle as a bearing stiffener beneath the floor joist in a CFS framing system is shown in Fig. 1.

[1]Research Scholar, Dept. of Civil Engineering, Indian Institute of Technology Hyderabad, Kandi, Sangareddy, Telangana 502284, India. ORCID: https://orcid.org/0000-0002-1721-2355. Email: ce18resch11007@iith.ac.in

[2]Professor, Dept. of Civil Engineering, Indian Institute of Technology Hyderabad, Kandi, Sangareddy, Telangana 502284, India (corresponding author). ORCID: https://orcid.org/0000-0002-3144-5278. Email: mkm@ce.iith.ac.in

Note. This manuscript was submitted on May 18, 2022; approved on November 29, 2022; published online on March 13, 2023. Discussion period open until August 13, 2023; separate discussions must be submitted for individual papers. This paper is part of the ***Journal of Structural Engineering***, © ASCE, ISSN 0733-9445.

AISI (2016) design guidelines focus primarily on the load-carrying capacities of the individual fasteners like bolts, screws, and welds, rather than the clip-angle. However it is also important to analyze the behavior and evaluate the shear capacity of the clip-angle. Considerable research has been conducted (Natesan et al. 2020, 2021; Natesan and Madhavan 2019; Obeydi et al. 2020, 2021; Redwood and Eyre 1984; Fox 2005; Yam et al. 2007a, b; Yu et al. 2017, 2018, 2016; Zhang et al. 2018, 2022) on clip-angles under different loading conditions by varying connection types (screws, bolts, and weld) and geometric parameters (thickness, width, and depth). The application of clip-angle as stiffeners at bearing locations in a CFS framing system was thoroughly studied by Fox (2005). Yam et al. (2007a) experimentally investigated the block shear capacity of a welded HRS clip-angle, and then numerically validated the study (Yam et al. 2007b). A comprehensive review of cold-formed steel clip-angle subjected to different loading conditions such as shear, compression, and pull-over was performed by Yu et al. (2015). The study by Zhang et al. (2018) is further extended by Zhang et al. (2022) considering the service limit state of cold-formed steel connectors and the screw pattern effect of the design strength of the clip-angle.

The outcome of the Yu et al. (2016) work elucidated that clip-angle shear strength has a power law relation with its slenderness ratio. More specifically, clip-angle shear strength and compression capacity were evaluated through laboratory tests by Yu et al. (2016, 2017), while the pull-out capacity of a load-bearing clip-angle was extensively studied by Obeydi et al. (2020, 2021) through experimental investigation and numerical analysis, respectively. A clip-angle tensile capacity evaluation and service limit state design was carried out by Zhang et al. (2018). Extensive research into the shear strength of bolted clip-angles was conducted by Natesan et al. (2020) and Natesan and Madhavan (2019) for 2-bolt and 3-bolt configurations, respectively. Moreover, experimental analysis carried out by Natesan et al. (2021) to understand the effect of beam

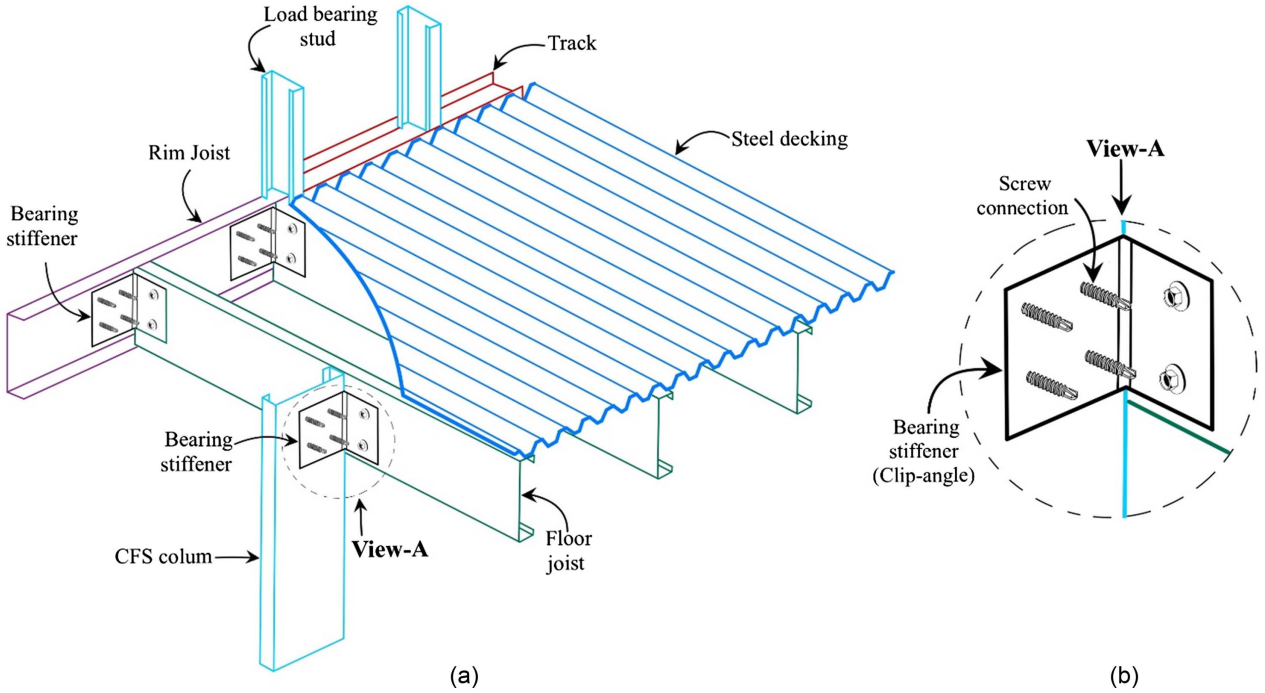

Fig. 1. CFS framing system: (a) typical view of CFS floor decking system; and (b) application of clip-angle as bearing stiffener.

depth on the ultimate shear capacity of clip-angles with 2-bolt and 3-bolt configurations. Most recently, Zhang et al. (2022) suggested an improved design shear equation for a clip-angle with a multi-line number of screws, and also suggested an alternative design method for the shear capacity of the clip-angle from a finite-element analysis of their experimental records. The ability of clip-angles to resist cyclic loading was evaluated by Redwood and Eyre (1984). The research of Zhang et al. (2022) and Natesan et al. (2021) suggest the need to improve the currently available clip-angle design guidelines for wider application of the design equations.

The objective of this paper is to experimentally analyze the behavior of clip-angle connections and determine the realistic shear capacity of a 3-bolt CFS clip-angle constructed from a commonly available steel grade (f_y = 275 MPa to 300 MPa); compare it to the design shear equation for high-grade steel (f_y = 375 MPa to 550 MPa) developed by Natesan et al. (2020); and propose a design shear equation for a wider range of steel grades (f_y = 275 MPa to 550 MPa); by considering available research data for the 3-bolt clip-angle. As the focus of the study is to determine the shear strength of the clip-angle connector, the diameter of the bolts and number of bolts for each clip-angle configuration were kept constant.

Research Motivations

- The previously-proposed shear strength equation for a 3-bolt clip-angle (Natesan et al. 2020) is applicable only for high-grade steel (f_y = 375 MPa to 550 MPa).
- In the Natesan et al. (2020) study, some clip-angle configurations were omitted when developing the design shear equation due to premature beam bearing failure. Therefore, the shear capacity of some clip-angles remains elusive and the suggested shear equation may not be reliable.
- The suggested shear strength of a three bolt clip-angle configuration is applicable to a two bolt configuration as well, because the bolt pitch is also included as a parameter.

Material Test

Coupon Testing

The material properties of the clip-angle used in this study were determined from the coupon test on a 30 kN capacity Instron 5969 (Instron, Norwood, Massachusetts) universal testing machine. The coupons as shown in Fig. 2 were cut from the flat portion of the outstanding leg of the clip-angle. All coupons were tested with a displacement loading rate of 0.01 mm/s according to ASTM E8/E8M-13a (ASTM 2010) and Huang and Young (2014), and the results are tabulated in Table 1. The material test results are plotted in Fig. 3.

Labelling of Test Specimens and Specimen Details

The test specimens were labeled as illustrated in Fig. 4. The clip-angle leg connected to the supporting member (column) is called an outstanding leg, while the other leg is attached to the loaded member (beam or loading plate) referred to as loathe ding leg as shown in Fig. 5(c). The ultimate shear strength of the clip-angle was studied by varying the clip-angle thickness (1.5 mm, 2 mm, and 2.5 mm), depth (150 mm and 180 mm), and width (65 mm, 95 mm, and 125 mm). The combined effect of depth and thickness was studied with a factor called aspect ratio (L/D), where L is the flat length of the out-standing leg and D is the depth of the clip-angle. The flat length was measured from the inner fold line of the outstanding leg to the bolt center line as shown in Fig. 5. Accordingly, the test specimen 2-65-150-3B-F2 indicates a clip-angle of the thickness of 2 mm, outstanding leg width of 65 mm, depth of 150 mm with 3 bolts in a single line (3B) and it is the second

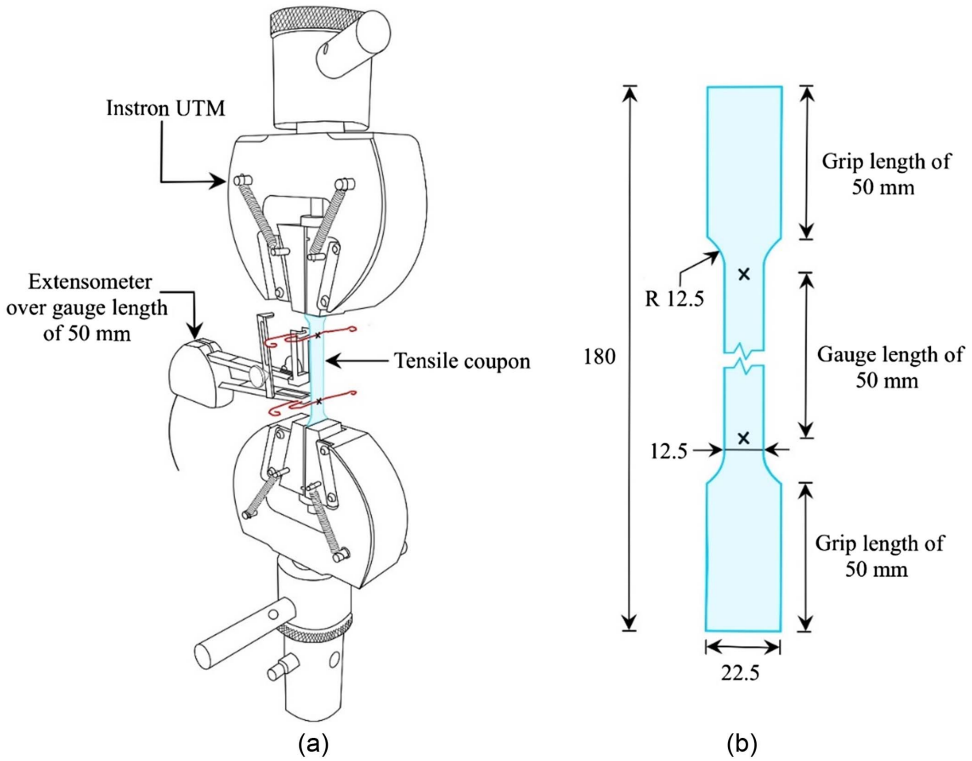

Fig. 2. Material test: (a) testing of the coupons on UTM; and (b) geometric layout of a steel coupon.

Table 1. Material test results

Thickness of clip-angle (mm)	Sample No.	Yield strength, f_y (N/mm^2)	Ultimate tensile strength, f_u (N/mm^2)	Ultimate strain (%)	Young's modulus, E (N/mm^2)
1.5	1	266.476	303.783	49.30	200,483
	2	274.120	299.129	45.50	201,925
	3	275.221	303.029	40.50	199,062
Mean		271.939	301.980	45.10	200,490
2	1	286.002	360.221	34.00	200,701
	2	282.088	355.869	33.50	200,664
	3	287.060	360.260	29.01	203,413
Mean		285.050	358.783	32.17	201,593
2.5	1	315.192	350.869	38.07	200,991
	2	301.848	366.408	36.51	199,367
	3	303.410	365.165	39.90	200,768
Mean		306.816	360.814	38.16	200,375

sample (F2) tested in fatigue testing machine (FTM). Failure of the loading leg was precluded by providing 4 bolts in it as shown in Fig. 5(c). The edge and pitch distance of bolts were maintained according to the AISI (2016) specifications.

Experimental Analysis

Phase-I Work

The in-plane transverse shear load was applied to the test samples with a displacement loading rate of 0.01 mm/s through a 16 mm thick HRS plate, as shown in Fig. 6(a). Two shear tests were conducted for each configuration of the clip-angle, followed by some repeat tests to check the consistency of the test results. The two shear tests (for the same clip-angle configuration) were found to have a good match with each other and variations in the ultimate shear strengths were found to be <10%, hence the experimental data was considered to be reliable. A built-up HRS base fixture, as shown in Fig. 6(b), was fabricated and a CFS column positioned in it. Threaded rods of 12 mm diameter were used to attach the CFS column to the HRS base fixture as shown in Fig. 6(a). An FTM-500 kN capacity machine was used for applying the displacement loading on the clip-angle. The vertical displacement of the clip-angle was measured by a linear variable differential transducer (LVDT) instrumented on the loading plate as shown in Fig. 7.

Ancillary Tests for Validation

Based on the literature (Natesan et al. 2020; Natesan and Madhavan 2019), the base of the CFS column was welded to an HRS plate (as shown in Fig. 8) to provide fixity to the column base. Although the base fixture used in the present research work appears to provide the same fixed boundary condition to the column base like in the CFS column base welded to HRS plate case, it needs to be verified. Hence some ancillary tests were conducted.

1.5-90-180 and 2-125-150 clip-angles were used in the ancillary tests and the results are illustrated in Fig. 9. In this section, test specimen identifier 1.5-90-180-V1-BB indicates the first validation test (V1) with column base bolted to the HRS base fixture [refer to Fig. 8(b)], while V2-BB indicates the second validation test with column base welded (BW) to HRS plate [refer Fig. 8(a)].

As shown in Fig. 9, the variation in ultimate shear strength of the test specimens was found to be <10% when the column base was welded to the HRS plate and bolted to the built-up base fixture. From the validation tests it can be concluded that the base fixture used in the present study was found to provide the same fixity to

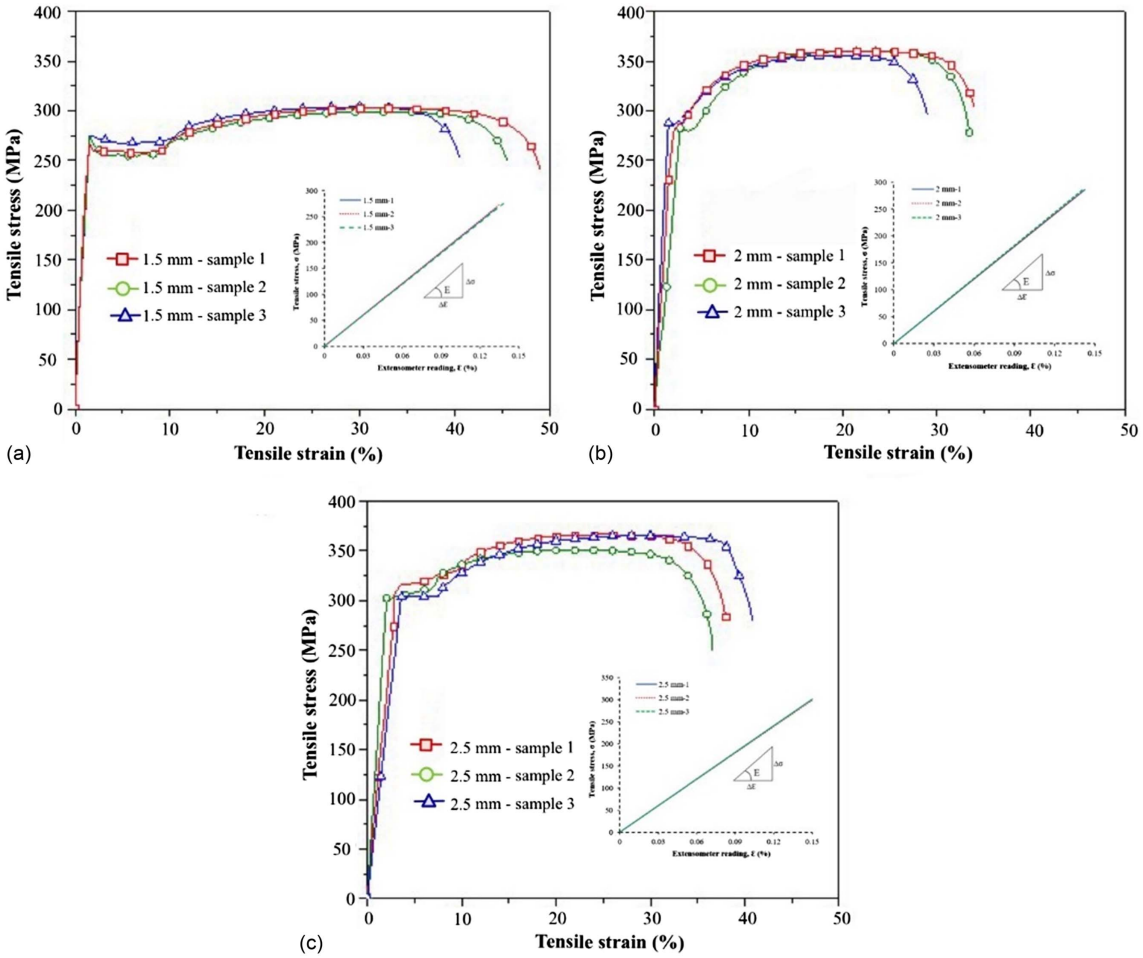

Fig. 3. Stress versus strain plots of tested coupons: (a) 1.5 mm thickness; (b) 2 mm thickness; and (c) 2.5 mm thickness.

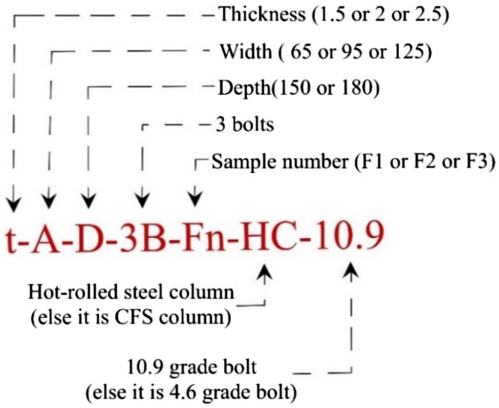

Fig. 4. Labeling of test specimens.

the column like in the welded base plate configuration; therefore, the base fixture can be used for test specimens.

In Phase-I experiments, most of the test specimens (27) experienced shear local buckling, while some of the test specimens (8) were subjected to column bearing failure. Contrary to other clip-angles that failed only in shear local buckling, the 1.5-65-180 clip-angle experienced tearing failure near the top-bolt portion along with shear local buckling, as shown in Fig. 10. Shear strength and displacement plots of Phase-I work are shown in Fig. 11 and results are provided in Table 2.

The initial stiffness of the clip-angle was found to decrease with an increase in its flat width from 65 mm to 95 mm and 125 mm. The high flat-width results in more out-of-plane movement of the outstanding leg of the clip-angle. Moreover, the increased flat width results in a higher aspect ratio of the outstanding leg of the clip-angle. Hence the clip-angle is subjected to early local buckling, which results in decreased ultimate shear strength and stiffness.

In the case of 1.5 mm thick and 150 mm depth clip-angles; a higher decrease in initial stiffness was observed when the flat width increased from 65 mm to 95 mm (6.38 kN/mm to 3.15 kN/mm) than that of the flat width increase from 95 mm to 125 mm (3.15 kN/mm to 1.70 kN/mm). The same trend was found in the case of the 1.5 mm thick and 180 mm depth clip-angles, while it was not observed in the 2 mm and 2.5 mm thick clip-angle test specimens due to premature column bearing failure. All the test specimens that were subjected to column bearing failure were found to have an aspect ratio of <0.23. The actual shear capacity of these test specimens is remain elusive. The actual shear capacity of the test specimens that were subjected to column bearing failure is unknown.

Phase-II Work

To determine the actual shear capacity of the clip-angles that experienced column bearing failure in Phase-I (refer to Table 2), the CFS column in the test specimen was replaced with a built-up HRS column made of 12 mm thick HRS plates, as shown in Fig. 12(a).

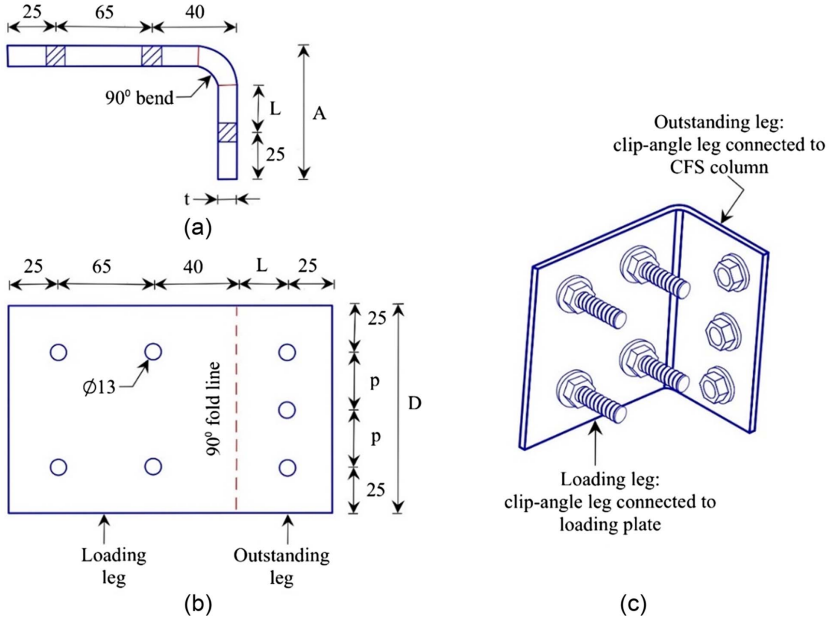

Fig. 5. Clip-angle views: (a) tOP-view; (b) flat-view; and (c) 3D-view.

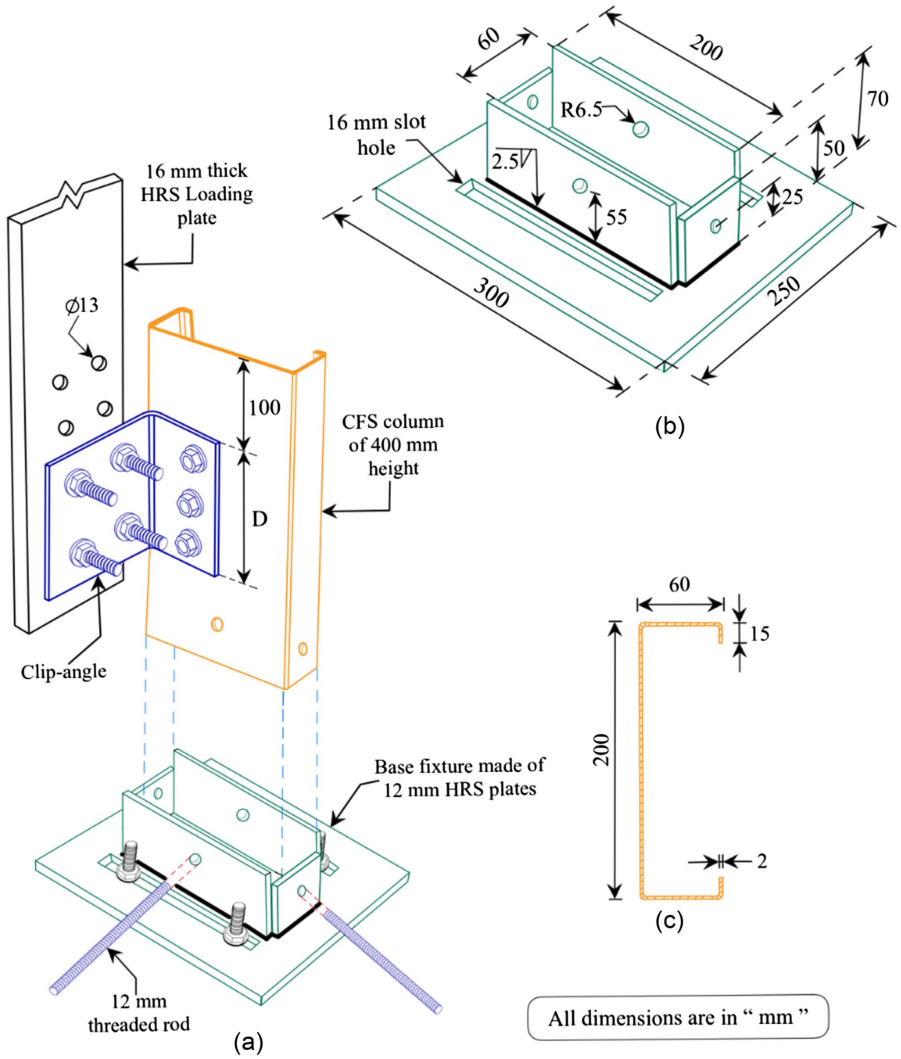

Fig. 6. Test set-up details: (a) installation of test specimen into base fixture; (b) base fixture for column; and (c) cross-section of CFS column.

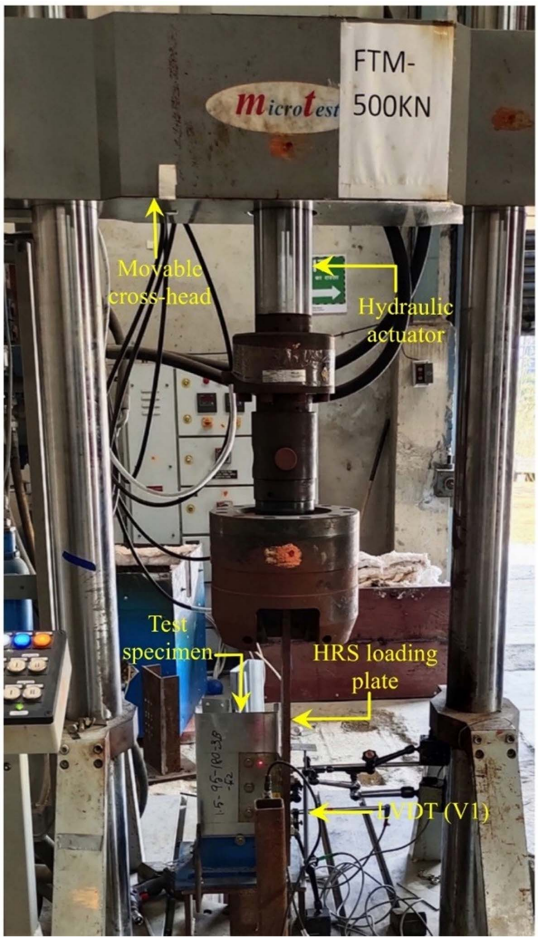

Fig. 7. Test setup and instrumentation.

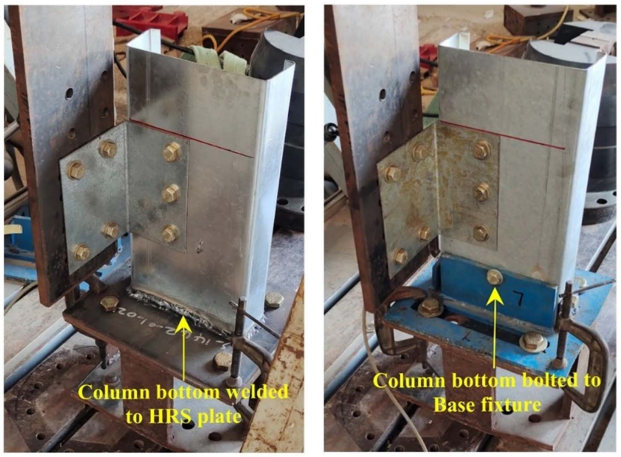

Fig. 8. Boundary conditions of test specimen: (a) column base welded; and (b) column base bolted to base fixture.

Experimental outcomes of the Phase-II work are illustrated in Fig. 13 and tabulated in Table 3. The 2-65-150 clip-angles were found to have tearing failure, while other specimens exhibited bolt shear failure, as shown in Fig. 12(b), and hence the actual shear capacity of the latter clip-angles is unknown.

In the case of the 2-65-150 clip-angles (see Fig. 13) no considerable variation in initial stiffness and ultimate shear strength was found in Phase II after replacing the CFS column with the HRS column. Hence, it can be concluded that the 2-65-150 clip-angle reached its ultimate shear strength before the column failure. But, for the 2-65-180 clip-angles, a considerable increase in ultimate shear strength (53.6 kN in Phase-I, 63.4 kN in Phase-II) was found, along with a marginal variation in initial stiffness (see Fig. 13). Though column failure was not observed in the 2-65-180 clip-angle after replacing the CFS column with the HRS column (in Phase-II), bolt shear failure did occur, which makes Phase-II results unreliable in predicting the shear capacity of the clip-angles. Bolt shear failure (sudden load in Fig. 13) was also observed in the 2.5-65-150 and 2.5-65-180 clip-angles.

Phase-III Work

To determine the actual shear capacity of the clip-angles that experienced bolt shear failure in the Phase-II experiments, in Phase-III 4.6 grade bolts were replaced with 10.9-grade high strength bolts to preclude bolt failure, as shown in Fig. 14. The results of the Phase-III experiments are shown in Fig. 15 and Table 4. In the Phase-III experiments all the clip-angles failed by plate tearing.

For the 2-65-180 clip-angle (refer to Fig. 15) no considerable variation in ultimate shear strength and initial stiffness was found after replacing the 4.6 grade bolt with 10.9-grade bolts, while a <10% variation in ultimate shear strength was found in the Phase-II and Phase-III results for the 2.5-65-150 clip-angles. Hence the Phase-II and Phase-III test results of 2-65-180 and 2.5-65-150 were considered in developing the design shear equation. A considerable variation (21%) in ultimate shear strength was found for the 2.5-65-180 clip-angle after using 10.9-grade bolts (87.21 kN in Phase-II, 105.37 kN in Phase-III); hence, Phase-II test results were omitted.

Parametric Study

Width Effect

As the width of the clip-angle increases, its ultimate shear strength decreases due to the out-plane bending of the clip-angle. A 38% to 54% decrease in shear strength was observed in the clip-angles when the flat width was increased from 65 mm to 95 mm, and a further 14% to 31% decrease in shear strength was observed when the flat width was increased to 125 mm (refer to Table 5 and Fig. 16).

Thickness Effect

As the thickness of the clip-angle increases its ultimate shear strength increases. As shown in Table 6, when thickness increases from 1.5 mm to 2 mm the increase in ultimate shear strength was higher in the case of 150 mm depth clip-angles (70% to 202%) than that of 180 mm depth clip-angles (59% to 69%). However, for the further increase of thickness from 2 mm to 2.5 mm the shear strength increase was approximately equal for both 150 mm (67% to 140%) and 180 mm (75% to 121%) clip-angles.

Depth Effect

As the depth of the clip-angle increases its ultimate shear strength increases due to the decreased aspect ratio (L/D) of the clip-angle (refer to Table 7). The high aspect ratio (0.64) and low thickness

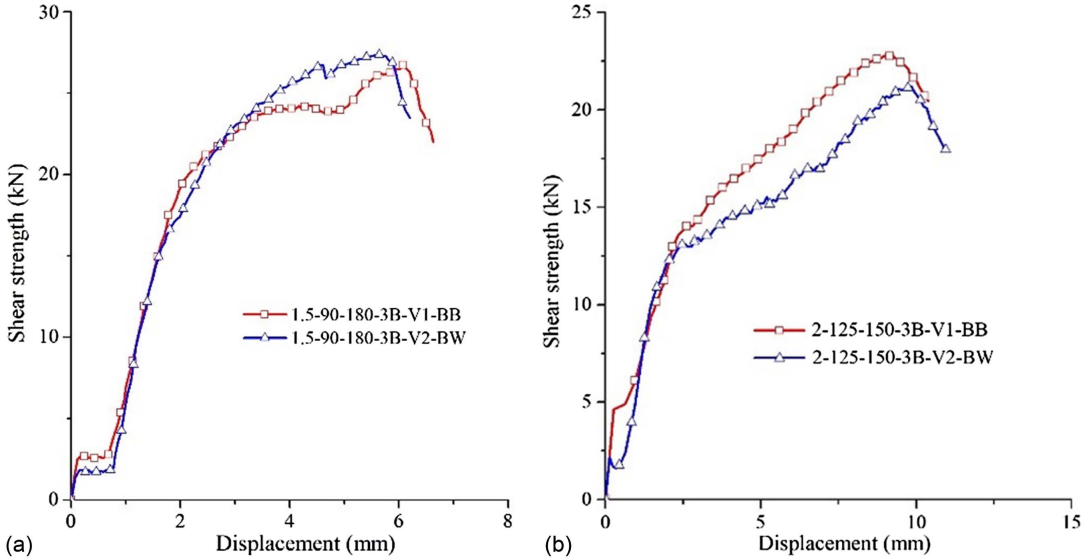

Fig. 9. Ancillary tests for validation of test set-up: (a) 1.5-95-180 clip-angle; and (b) 2-125-150 clip-angle.

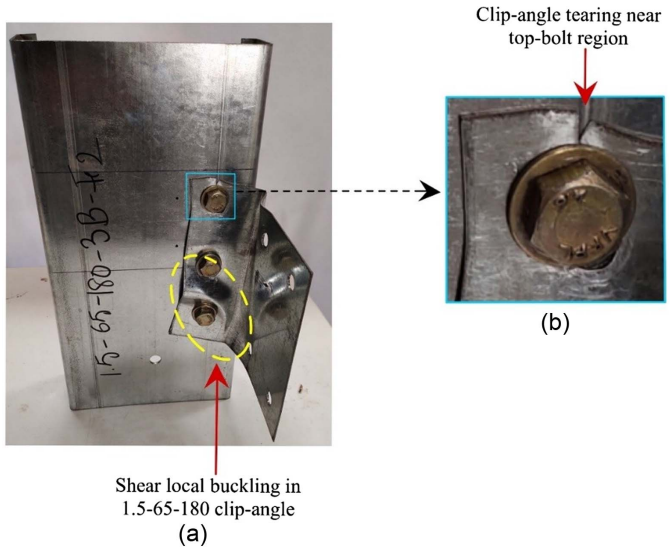

Fig. 10. Failure of 1.5-65-180 clip-angle: (a) severe shear local buckling; and (b) tearing in clip-angle.

(1.5 mm) of the 1.5-125-150 clip-angle make it highly unstable; hence a depth increase to 180 mm (1.5-125-180) causes the highest shear strength increment (95%). Except for 1.5-125-150, all remaining clip-angles have a marginal increase (9% to 39%) in shear strength when the depth increases from 150 mm to 180 mm. The highest aspect ratio (0.64) and lowest thickness (1.5 mm) of the 1.5-125-150 clip-angle make it highly unstable; hence the depth increase to 180 mm (1.5-125-180) causes the highest (95%) shear strength increment.

Failure Modes of Test Specimens

Shear Local Buckling of Clip-Angle

The unexpected failure modes such as column bearing failure and bolt shear failure in the test specimens were ignored while distinguishing the failure modes (Fig. 17) of the clip-angle as they caused premature failure of test specimens. Clip-angles with the aspect ratio $(L/D) > 0.23$ failed due to shear local buckling as shown in Fig. 18 while remaining clip-angles ($L/D \leq 0.23$) failed due to tearing of the outstanding leg the of clip-angle.

Column Bearing Failure

Column bearing failure was observed in the test specimens in Phase-I experiments (see Fig. 19). This is a result of compressive stress (bearing) developed at the bottom side of the clip-angle due to the rotation of the clip-angle. This compressive stress caused inward bearing failure in the column web portion and outward buckling failure of the column flange, as shown in Figs. 19(a and b), respectively. Hence the test specimens failed due to premature column failure.

Bolt Shear Failure and Plate Tear Failure

Tensile and compressive stresses developed in the clip-angles due to the shear deformation of the clip-angle, as shown in Fig. 20(b). These high principal stresses resulted in bolt shear failure of the Phase-II specimens indicating the high shear capacity of the clip-angle over the bolts provided. Hence 10.9-grade high strength bolts were used in the Phase-III experiments. This resulted in the tearing failure of the clip-angle, with no failure of the 10.9-grade bolts. All the clip-angles in the Phase-III tests experienced excessive deformation, which resulted in the formation of a diagonal band, as shown in Fig. 20(b). This is similar to the diagonal bands formed in a typical plate girder as a result of tension field action (TFA). Unlike a typical plate girder with stiffeners, the outstanding leg of the clip-angle was not stiffened, hence the TFA effect can be neglected.

Discussions

The following inferences are drawn from the observation of the failure modes of the clip-angles:

- Column failure can be precluded if the thickness of the column section is greater than or equal to the clip-angle thickness ($t_{\text{column}} > t_{\text{clip-angle}}$).
- Column failure occurred in the Phase-I work with a 2 mm thick CFS column, while bolt shear failure occurred okin Phase-II work with a 12 mm HRS column. This indicates the high strength

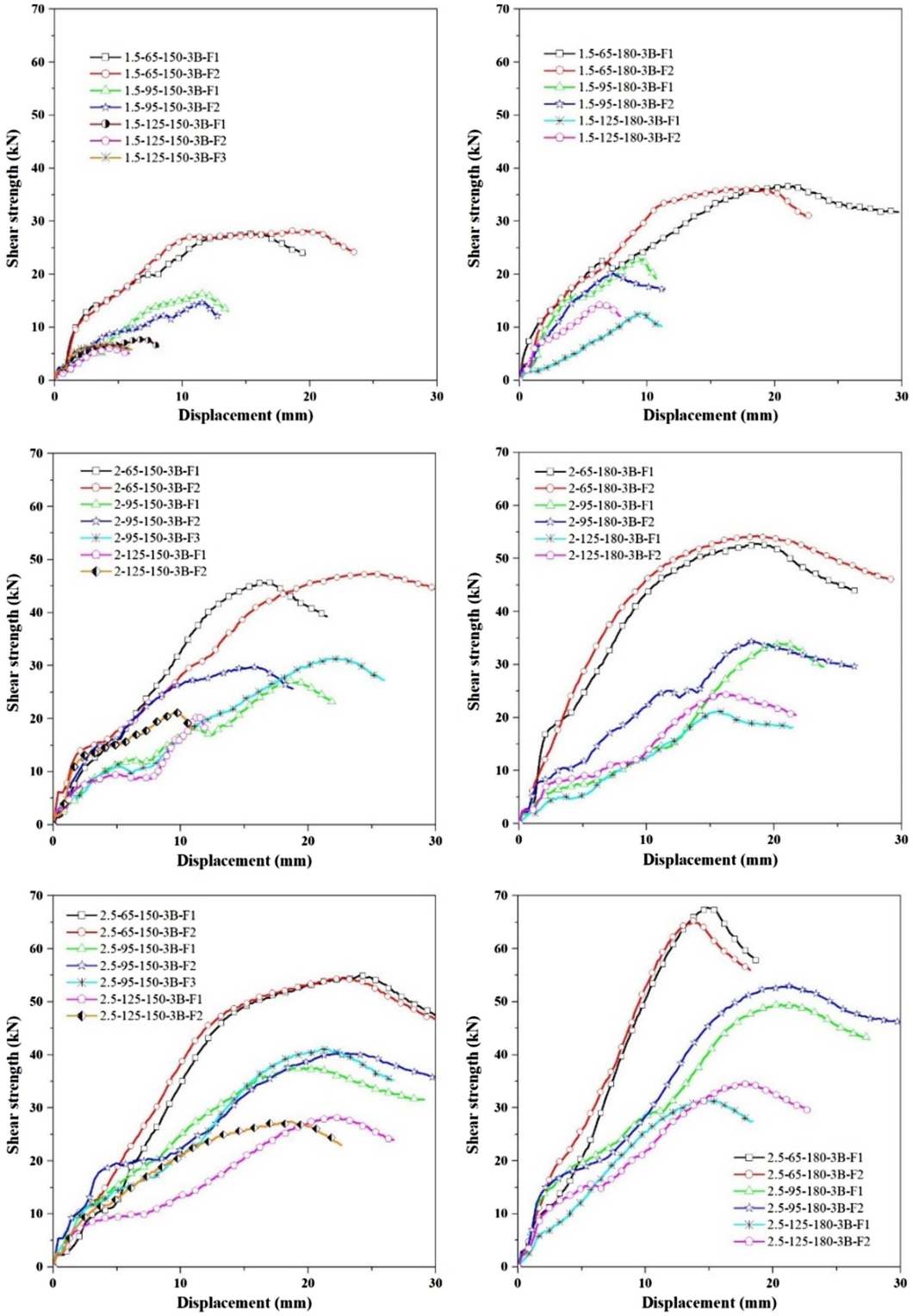

Fig. 11. Shear strength versus displacement plots of Phase-I work.

of the CFS clip-angle, hence the 3-bolt CFS clip-angle is recommended in hybrid steel structures.

- From Fig. 17, an aspect ratio $(L/D) > 0.23$ is recommended to preclude the supporting member (CFS column) failure and fastener (bolts) failure in the case of a 3-bolt clip-angle. Commonly-used M4.6 grade bolts are not recommended if $(L/D) \leq 0.23$, as the clip-angle undergoes failure due to fracture.

Design Shear Equation

Applicability of Existing Design Shear Equation

The shear strength equation proposed by Natesan et al. (2020) for the 3-bolt clip-angle for a steel grade of 375 MPa to 550 MPa, by Natesan and Madhavan (2019) for the 2-bolt clip-angle, and

Table 2. Experimental outcomes of Phase-I work

S. No.	Clip-angle configuration: *t-A-D*	Ultimate shear strength, V_{exp} (kN)	Failure mode	Aspect ratio (L/D)
1	1.5-65-150-3B-F1	27.69	SLB	0.24
2	1.5-65-150-3B-F2	28.27	SLB	0.24
3	1.5-95-150-3B-F1	16.3	SLB	0.44
4	1.5-95-150-3B-F2	14.62	SLB	0.44
5	1.5-125-150-3B-F1	7.75	SLB	0.64
6	1.5-125-150-3B-F2	6.12	SLB	0.64
7	1.5-65-180-3B-F1	36.67	f Tearing	0.20
8	1.5-65-180-3B-F2	36.17	SLB+Tearing	0.20
9	1.5-95-180-3B-F1	22.91	SLB	0.37
10	1.5-95-180-3B-F2	20.17	SLB	0.37
11	1.5-125-180-3B-F1	12.6	SLB	0.53
12	1.5-125-180-3B-F2	14.4	SLB	0.53
13	2-65-150-3B-F1	45.67	SLB+CF	0.23
14	2-65-150-3B-F2	47.37	SLB+CF	0.23
15	2-95-150-3B-F1	27.14	SLB	0.43
16	2-95-150-3B-F2	29.76	SLB	0.43
17	2-125-150-3B-F1	20.59	SLB	0.63
18	2-125-150-3B-F2	21.21	SLB	0.63
19	2-65-180-3B-F1	52.84	SLB+CF	0.19
20	2-65-180-3B-F2	54.3	SLB+CF	0.19
21	2-95-180-3B-F1	34.04	SLB	0.36
22	2-95-180-3B-F2	34.34	SLB	0.36
23	2-125-180-3B-F1	21.18	SLB	0.53
24	2-125-180-3B-F2	24.49	SLB	0.53
25	2.5-65-150-3B-F1	55.05	SLB+CF	0.23
26	2.5-65-150-3B-F2	54.33	SLB+CF	0.23
27	2.5-95-150-3B-F1	37.63	SLB	0.43
28	2.5-95-150-3B-F2	40.32	SLB	0.43
29	2.5-125-150-3B-F1	28.2	SLB	0.63
30	2.5-125-150-3B-F2	27.36	SLB	0.63
31	2.5-65-180-3B-F1	67.68	SLB+CF	0.19
32	2.5-65-180-3B-F2	65.21	SLB+CF	0.19
33	2.5-95-180-3B-F1	49.48	SLB	0.35
34	2.5-95-180-3B-F2	52.96	SLB	0.35
35	2.5-125-180-3B-F1	31.44	SLB	0.52
36	2.5-125-180-3B-F2	34.54	SLB	0.52
37	1.5-125-150-3B-F3	6.86	SLB	0.64
38	2-95-150-3B-F3	31.4	SLB	0.43
39	2.5-95-150-3B-F3	41.05	SLB	0.43

Note: SLB = shear local buckling; and CF = column bearing failure.

by Zhang et al. (2022) for the multi-line screw clip-angles, are, respectively

$$V^1_{n3B} = 0.299(\lambda)^{-0.77} \times V_y \quad (1a)$$

$$V^1_{n2B} = 0.222(\lambda)^{-0.6} \times V_y \quad (1b)$$

$$V_{\text{screw}} = 0.45(\lambda)^{-0.5} \times V_y \quad (1c)$$

Most recently, Natesan et al. (2021) conducted an experimental program on 230 mm depth clip-angles with 2-bolt and 3-bolt configurations. In that study, the existing shear equations [Eqs. (1*a*) and (1*b*)] for the 180 mm depth clip-angles were found to apply to 230 mm depth clip-angles as well. Hence, Natesan et al. (2021) suggested no design equations.

In the present study, the clip-angle has a steel grade in the range of 275 MPa to 307 MPa. The present experimental outcomes of low-grade steel clip-angle (f_y = 275 MPa to 307 MPa) were compared with the design shear strength equation suggested for high-grade steel (f_y = 375 MPa to 550 MPa) clip-angle by Natesan et al. (2020), 2-bolt shear equation by Natesan and Madhavan (2019), and shear strength equation proposed by Zhang et al. (2022) for the screwed clip-angle configuration. From Table 8 and Fig. 21, it can be concluded that the previously proposed shear strength equation (Natesan et al. 2020) results in highly conservative shear strength values for clip-angles in commonly available steel grades (f_y = 275 MPa to 307 MPa). Moreover, in developing their design shear strength equation, Natesan et al. (2020) omitted some clip-angles due to beam bearing failure of the test specimens. Therefore, the actual shear strength of those clip-angles remains elusive. This means that the previously proposed shear strength equation for the 3-bolted clip-angle yields conservative results (Fig. 21) for the low-grade steel and inaccurate results for some clip-angles of high-grade steel. Though the diameter of the bolt was kept constant, the pitch was varied in the 3-bolt clip-angle configuration in 150 mm and 180 mm depths. However, the shear strength equation suggested by Natesan et al. (2020) did not consider the bolt pitch in developing the shear strength equation for the 3-bolt clip-angle. The shear strength equation suggested by Zhang et al. (2022)

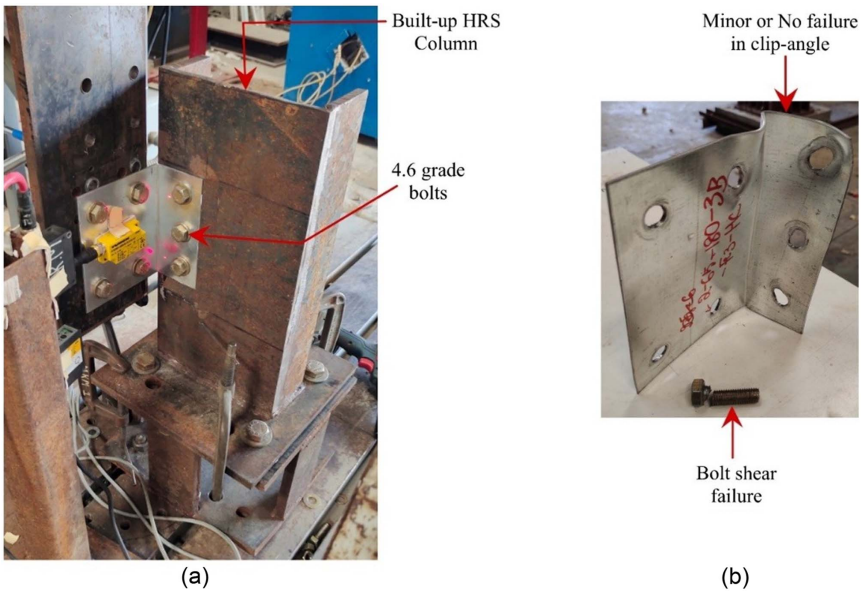

Fig. 12. Phase-II work: (a) HRS column test setup; and (b) bolt shear failure with minor or no failure in clip-angle.

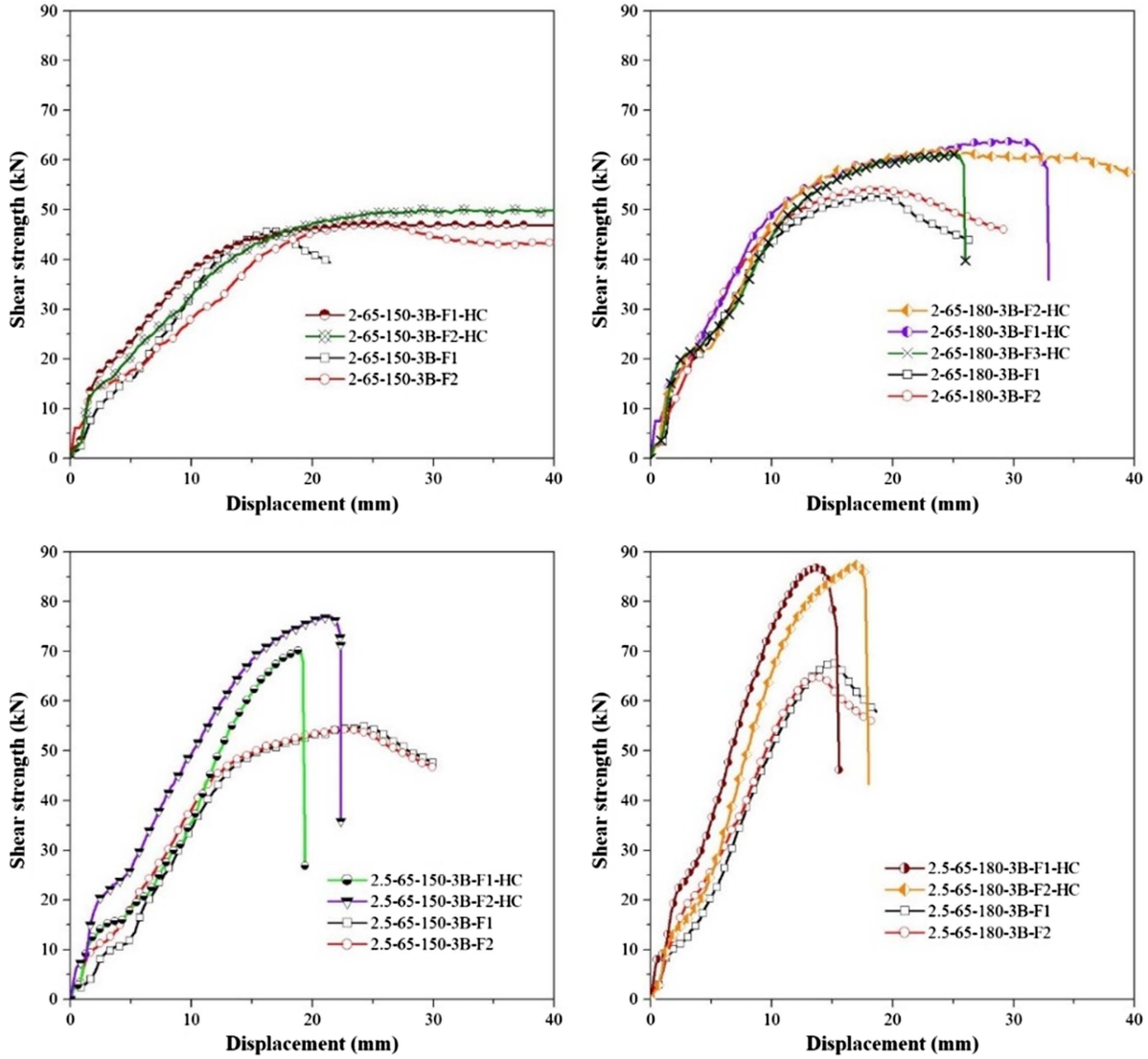

Fig. 13. Shear strength versus displacement plots of Phase-II work.

Table 3. Experimental outcomes of Phase-II work

S. No.	Clip-angle configuration: *t*-*A*-*D*	Ultimate shear strength, V_{exp} (kN)	Failure mode	Aspect ratio (L/D)
1	2-65-150-3B-F1-HC	47.08	Clip-angle tear failure	0.23
2	2-65-150-3B-F2-HC	50.03	Clip-angle tear failure	0.23
3	2-65-180-3B-F1-HC	63.9	Clip-angle tear failure	0.19
4	2-65-180-3B-F2-HC	62.05	Bolt shear failure	0.19
5	2-65-180-3B-F3-HC	61.16	Bolt shear failure	0.19
6	2.5-65-150-3B-F1-HC	70.43	Bolt shear failure	0.23
7	2.5-65-150-3B-F2-HC	77.05	Bolt shear failure	0.23
8	2.5-65-180-3B-F1-HC	87.05	Bolt shear failure	0.19
9	2.5-65-180-3B-F2-HC	87.37	Bolt shear failure	0.19

overestimates while the Natesan and Madhavan (2019) 2-bolt shear equation highly underestimates, when compared with the shear strength of the 3-bolt clip-angles shown in Fig. 21. Hence, a new design shear strength equation was developed using the present experimental data and the curve fitting method. The bolt pitch was included as a variable (refer to Fig. 24 in Appendix I), while the bolt diameter (12 mm) was kept constant. A new shear strength equation considering the bolt pitch, which is applicable for the 3-bolt and 2-bolt clip-angle configurations, is proposed from the experimental data. Out of 54 experiments, six test specimens experienced unexpected failures (column failure and bolt shear failure) resulting in the underestimation of clip-angle shear strength. Therefore, only 48 test results were considered in the development of the new shear strength equation. The new shear strength equation suggested for the bolted (3-bolt and 2-bolt) clip-angle connector considering the bolt pitch is

$$V_{3B/2B} = 0.12\left(\frac{p}{D}\lambda\right)^{-0.88} V_y \tag{2}$$

where p = bolt pitch; D = depth of the clip-angle; λ = slenderness ratio of the clip-angle; and V_y = yield shear strength of the clip-angle.

The limits of applicability are:

- Configuration: bolted clip-angle subjected to shear load.
- Clip-angle thickness: from 1.5 mm to 2.5 mm.
- Material yield strength: from 275 to 550 MPa.
- Maximum depth of the CFS beam: 200 mm.
- Aspect ratio (L/D) of out-standing leg: from 0.19 to 0.64.

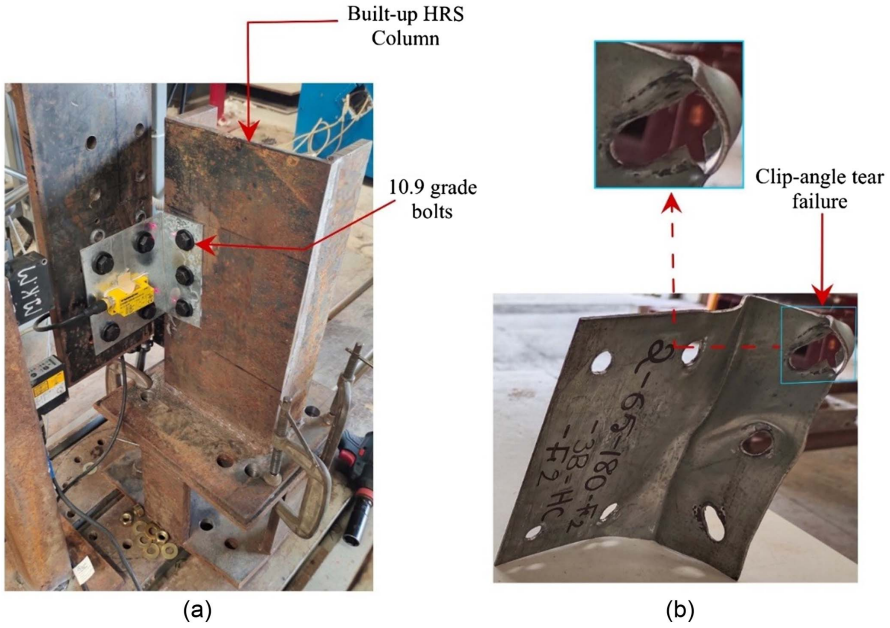

Fig. 14. Phase-III work: (a) HRS column and 10.9-grade bolts test setup; and (b) clip-angle tear failure with no bolt failure.

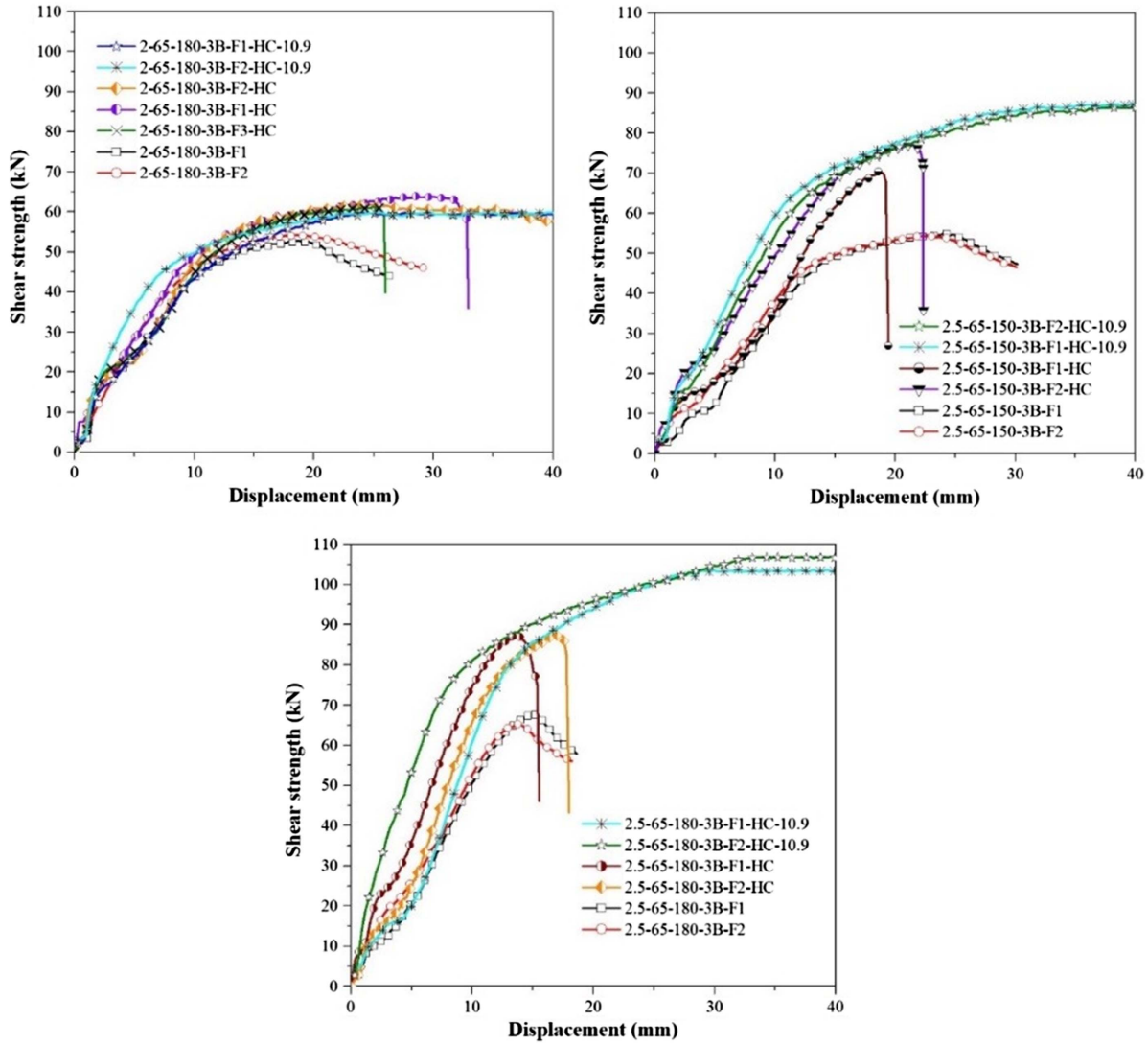

Fig. 15. Shear strength versus displacement plots of Phase-III work.

Table 4. Experimental outcomes of Phase-III work

S. No.	Clip-angle configuration: *t-A-D*	Ultimate shear strength, V_{exp} (kN)	Failure mode	Aspect ratio (L/D)
1	2-65-180-3B-F1-HC-10.9	59.79	Clip-angle tear failure	0.19
2	2-65-180-3B-F2-HC- 10.9	59.80	Clip-angle tear failure	0.19
3	2.5-65-150-3B-F1-HC-10.9	87.21	Clip-angle tear failure	0.23
4	2.5-65-150-3B-F2-HC- 10.9	86.29	Clip-angle tear failure	0.23
5	2.5-65-180-3B-F1-HC-10.9	103.68	Clip-angle tear failure	0.19
6	2.5-65-180-3B-F2-HC- 10.9	107.06	Clip-angle tear failure	0.19

Table 5. Width effect on ultimate shear strength of 3-bolt clip-angle

Thickness, t (mm)	Depth, D (mm)	Width, A (mm)	Ultimate shear strength, V_{exp} (kN)	% decrease in ultimate shear strength	% decremental decrease in ultimate shear strength
1.5	150	65	27.98	0	
		95	15.46	−45	
		125	6.91	−75	−31
	180	65	36.42	0	
		95	21.54	−41	
		125	13.50	−63	−22
2	150	65	47.54	0	
		95	29.31	38	
		125	20.90	−56	−18
	180	65	61.34	0	
		95	34.19	−44	
		125	22.84	−63	−19
2.5	150	65	86.75	0	
		95	39.66	−54	
		125	27.78	−68	−14
	180	65	105.37	0	
		95	51.22	−51	
		125	32.99	−69	−17

The new shear strength equation considering the bolt pitch was found to have a good match (refer to Table 8) with the experimental data of both the present 3-bolt clip-angle of low-grade steel and the Natesan et al. (2020) 3-bolt clip-angle of high-grade steel, with a mean of 1.06 and standard deviation of 0.15, as provided in Table 8.

Application of the Proposed Shear Equation for the 2-Bolt Clip-Angle

The shear strength equation for the 2-bolt clip-angle proposed by Natesan and Madhavan (2019) is

$$V^1_{n2B} = 0.222(\lambda)^{-0.6} \times V_y \tag{3}$$

As set forth in Table 9 and Fig. 22, the proposed new design equation [Eq. (2)] is in good agreement with the 2-bolt experimental data of Natesan and Madhavan (2019) [Eq. (3)], with little variation. Therefore, the proposed new shear strength equation is efficient for the 3-bolt as well as for the 2-bolt clip-angle configuration. From Tables 8 and 9 it can be concluded that the proposed equation for the 3-bolt configuration (present study and Natesan et al. 2020) and 2-bolt configuration (Natesan and Madhavan 2019) have a good match with experimental data, with a mean of 1.12 and standard deviation of 0.25.

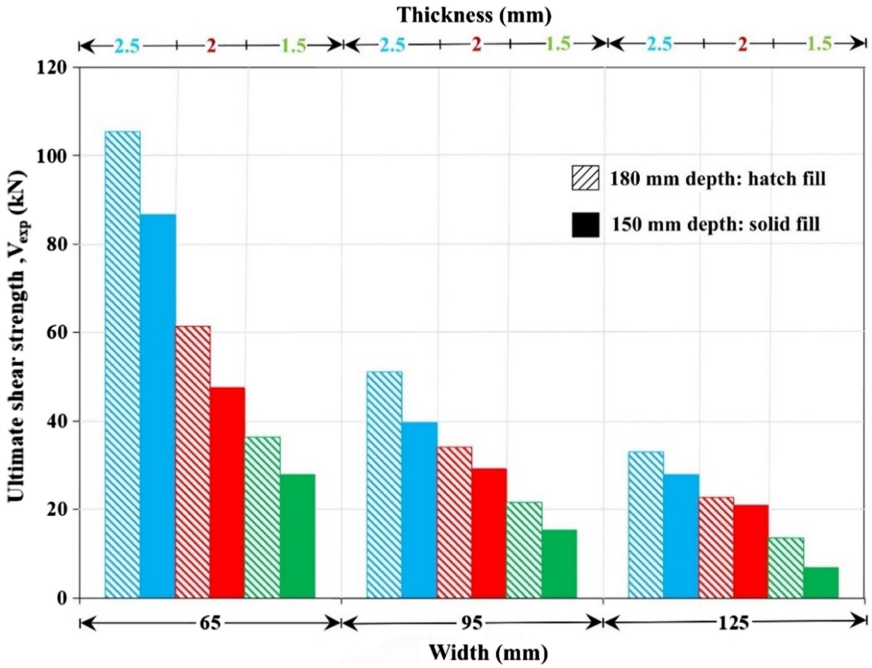

Fig. 16. Effect of clip-angle thickness, width, and depth on ultimate shear strength.

Table 6. Thickness effect on ultimate shear strength of 3-bolt clip-angle

Width, A (mm)	Depth, D (mm)	Thickness, t (mm)	Ultimate shear strength, V_{exp} (kN)	% Increase in ultimate shear strength	% Incremental increase in ultimate shear strength
65	150	1.5	27.98		
		2	47.54	70	
		2.5	86.75	210	140
95	150	1.5	15.46		
		2	29.31	90	
		2.5	39.66	157	67
125	150	1.5	6.91		
		2	20.90	202	
		2.5	27.78	302	100
65	180	1.5	36.42		
		2	61.34	68	
		2.5	105.37	189	121
95	180	1.5	21.54		
		2	34.19	59	
		2.5	51.22	138	79
125	180	1.5	13.50		
		2	22.84	69	
		2.5	32.99	144	75

Table 7. Depth effect on ultimate shear strength of 3-bolt clip-angle

Thickness, t (mm)	Width, W (mm)	Depth, D (mm)	Aspect ratio (L/D)	Ultimate shear strength, V_{exp} (kN)	% Increase in ultimate shear strength
1.5	65	150	0.24	27.98	
		180	0.20	36.42	30
	95	150	0.44	15.46	
		180	0.37	21.54	39
	125	150	0.64	6.91	
		180	0.53	13.50	95
2	65	150	0.23	47.54	
		180	0.19	61.34	29
	95	150	0.43	29.31	
		180	0.36	34.19	17
	125	150	0.63	20.90	
		180	0.53	22.84	9
2.5	65	150	0.23	86.75	
		180	0.19	105.37	21
	95	150	0.43	39.66	
		180	0.35	51.22	29
	125	150	0.63	27.78	
		180	0.52	32.99	19

The increase in the ultimate shear strength of a clip-angle with the addition of a bolt was investigated (Table 10 and Fig. 23) by comparing the test results of the present study (3-bolt configuration) and the previously proposed empirical shear equation of Natesan and Madhavan (2019) for the 2-bolt configuration.

From the comparative study of the 3-bolt and 2-bolt configurations of clip-angle (refer to Table 10), it can be concluded that the ultimate shear strength significantly increased with the addition of a bolt to the clip-angle (refer to Appendixes I–IV). This increase

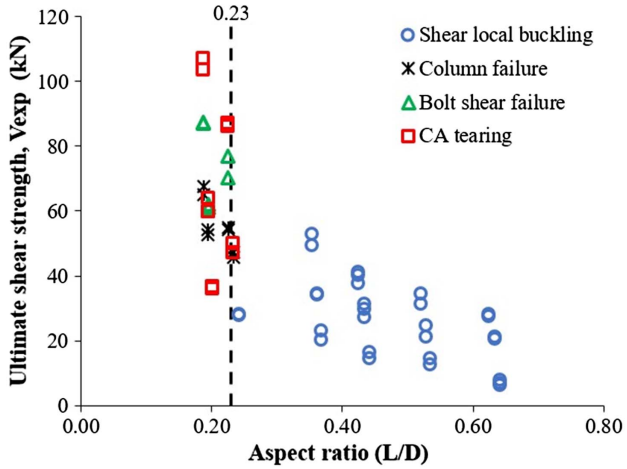

Fig. 17. Failure modes of test specimens.

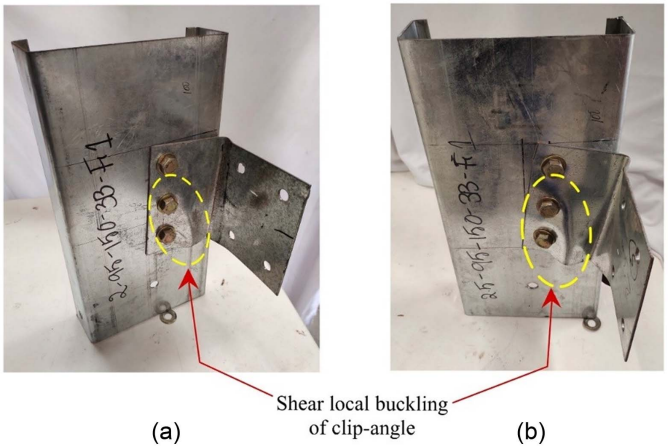

Fig. 18. Shear local buckling in specimens: (a) 2-95-150-3B-F1; and (b) 2.5-95-150-3B-F1.

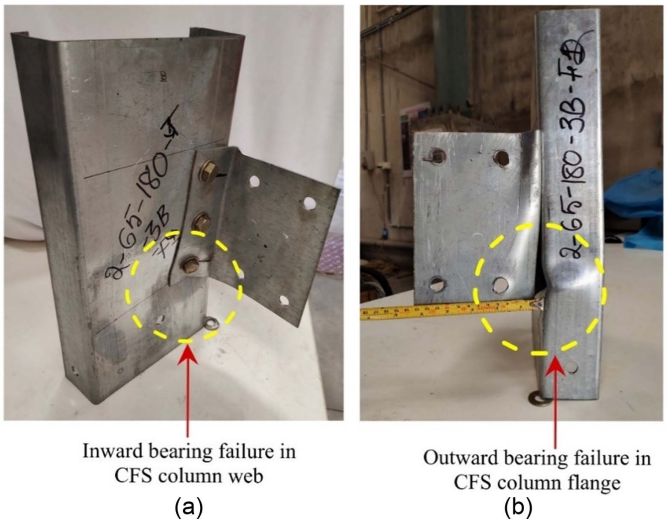

Fig. 19. Column bearing failure: (a) inward bearing failure in CFS column web; and (b) outward buckling of CFS column flange.

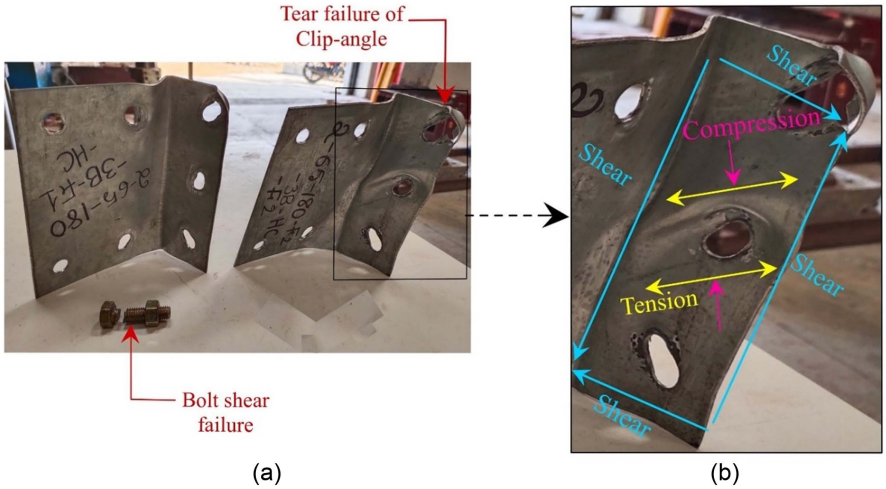

Fig. 20. Failure modes in clip-angle: (a) bolt shear failure and CA tearing; and (b) failure mechanism of CA tearing.

Table 8. Suggested novel shear strength equation by curve fitting

S. No.	Clip-angle configuration: *t-A-D*	Phase	$\frac{p}{D}\lambda$	$V_{\exp}$ (kN)	Natesan et al. $(V^1_{n3B}) = 0.299\,(\lambda)^{-0.77} V_y$ (kN)	$\frac{V_{\exp}}{V^1_{n3B}}$	Proposed shear strength $(V_{n-3B}) = 0.12(\lambda p/D)^{-0.88}\, V_y$ (kN)	$\frac{V_{\exp}}{V_{n-3B}}$
1	1.5-65-150-3B-F1	I	0.13	27.69	22.53	1.23	26.36	1.05
2	1.5-65-150-3B-F2	I	0.13	28.27	22.53	1.25	26.36	1.07
3	1.5-95-150-3B-F1	I	0.25	16.3	13.51	1.21	14.70	1.11
4	1.5-95-150-3B-F2	I	0.25	14.62	13.51	1.08	14.70	0.99
5	1.5-125-150-3B-F1	I	0.38	7.75	9.84	0.79	10.23	0.76
6	1.5-125-150-3B-F2	I	0.38	6.12	9.84	0.62	10.23	0.60
7	1.5-65-180-3B-F1	I	0.14	36.67	27.42	1.34	29.96	1.22
8	1.5-65-180-3B-F2	I	0.14	36.17	27.42	1.32	29.96	1.21
9	1.5-95-180-3B-F1	I	0.27	22.91	16.45	1.39	16.70	1.37
10	1.5-95-180-3B-F2	I	0.27	20.17	16.45	1.23	16.70	1.21
11	1.5-125-180-3B-F1	I	0.41	12.6	11.98	1.05	11.63	1.08
12	1.5-125-180-3B-F2	I	0.41	14.4	11.98	1.20	11.63	1.24
13	2-65-150-3B-F1	I	0.10	45.67	39.92	1.14	48.29	0.95
14	2-65-150-3B-F2	I	0.10	47.37	39.92	1.19	48.29	0.98
15	2-95-150-3B-F1	I	0.19	27.14	23.62	1.15	26.51	1.02
16	2-95-150-3B-F2	I	0.19	29.76	23.62	1.26	26.51	1.12
17	2-125-150-3B-F1	I	0.29	20.59	17.12	1.20	18.35	1.12
18	2-125-150-3B-F2	I	0.29	21.21	17.12	1.24	18.35	1.16
19	2-65-180-3B-F1	I	0.10	52.84	48.59	1.09	54.89	0.96
20	2-65-180-3B-F2	I	0.10	54.3	48.59	1.12	54.89	0.99
21	2-95-180-3B-F1	I	0.20	34.04	28.75	1.18	30.13	1.13
22	2-95-180-3B-F2	I	0.20	34.34	28.75	1.19	30.13	1.14
23	2-125-180-3B-F1	I	0.31	21.18	20.84	1.02	20.86	1.02
24	2-125-180-3B-F2	I	0.31	24.49	20.84	1.18	20.86	1.17
25	2.5-95-150-3B-F1	I	0.16	37.63	37.22	1.01	42.73	0.88
26	2.5-95-150-3B-F2	I	0.16	40.32	37.22	1.08	42.73	0.94
27	2.5-125-150-3B-F1	I	0.24	28.2	26.84	1.05	29.40	0.96
28	2.5-125-150-3B-F2	I	0.24	27.36	26.84	1.02	29.40	0.93
29	2.5-95-180-3B-F1	I	0.16	49.48	45.30	1.09	48.56	1.02
30	2.5-95-180-3B-F2	I	0.16	52.96	45.30	1.17	48.56	1.09
31	2.5-125-180-3B-F1	I	0.25	31.44	32.67	0.96	33.42	0.94
32	2.5-125-180-3B-F2	I	0.25	34.54	32.67	1.06	33.42	1.03
33	1.5-125-150-3B-F3	I	0.38	6.86	9.84	0.70	10.23	0.67
34	2-95-150-3B-F3	I	0.19	31.4	23.62	1.33	26.51	1.18
35	2.5-95-150-3B-F3	I	0.16	41.05	37.22	1.10	42.73	0.96
36	2-65-150-3B-F1-HC	II	0.10	47.08	39.92	1.18	48.29	0.97
37	2-65-150-3B-F2-HC	II	0.10	50.03	39.92	1.25	48.29	1.04
38	2-65-180-3B-F1-HC	II	0.10	63.9	48.59	1.32	54.89	1.16
39	2-65-180-3B-F2-HC	II	0.10	62.05	48.59	1.28	54.89	1.13
40	2.5-65-150-3B-F1-HC	II	0.08	70.43	63.82	1.10	79.12	0.89
41	2.5-65-150-3B-F2-HC	II	0.08	77.05	63.82	1.21	79.12	0.97

Table 8. (*Continued.*)

S. No.	Clip-angle configuration: *t-A-D*	Phase	$\frac{p}{D}\lambda$	V_{exp} (kN)	Natesan et al. $(V^1_{n3B}) = 0.299\,(\lambda)^{-0.77}V_y$ (kN)	$\frac{V_{exp}}{V^1_{n3B}}$	Proposed shear strength $(V_{n-3B}) = 0.12(\lambda p/D)^{-0.88}\,V_y$ (kN)	$\frac{V_{exp}}{V_{n-3B}}$
42	2-65-180-3B-F3-HC	II	0.10	61.16	48.59	1.26	54.89	1.11
43	2-65-180-3B-F1-HC-10.9	III	0.10	59.79	48.59	1.23	54.89	1.09
44	2-65-180-3B-F2-HC-10.9	III	0.10	59.8	48.59	1.23	54.89	1.09
45	2.5-65-150-3B-F1-HC-10.9	III	0.08	87.21	63.82	1.37	79.12	1.10
46	2.5-65-150-3B-F2-HC-10.9	III	0.08	86.29	63.82	1.35	79.12	1.09
47	2.5-65-180-3B-F1-HC-10.9	III	0.08	103.68	77.67	1.33	89.94	1.15
48	2.5-65-180-3B-F2-HC-10.9	III	0.08	107.06	77.67	1.38	89.94	1.19
For the present 48 test results					Mean	1.16		1.05
(f_y = 271 MPa to 307 MPa)					Standard deviation	0.16		0.14
					Coefficient variation	0.14		0.14
49	1.5-95-150	Natesan	0.36	32	18.94	1.53	21.84	1.46
50	1.5-125-150	et al.	0.54	18.4	12.09	1.21	15.21	1.21
51	1.5-95-180	(2020)	0.38	32.7	21.20	1.29	24.83	1.32
52	1.5-125-180		0.58	19.7	13.60	1.06	17.29	1.14
53	2-95-150		0.23	36.95	31.96	1.27	32.05	1.15
54	2-125-150		0.34	28.8	19.50	1.37	22.19	1.30
55	2-95-180		0.24	42.75	35.59	1.21	36.43	1.17
56	2-125-180		0.36	28.1	21.82	1.09	25.22	1.11
57	2.5-95-150		0.17	43	52.52	1.02	47.79	0.90
58	2.5-125-150		0.26	32.2	31.23	1.06	32.89	0.98
59	2.5-95-180		0.18	46.35	58.36	0.90	54.32	0.85
60	2.5-125-180		0.28	37.5	34.83	1.02	37.39	1.00
For the combined 60 test results					Mean	1.16		1.06
[present study and Natesan et al.					Standard deviation	0.16		0.15
(2020)] (f_y = 271 MPa to 550 MPa)					Coefficient variation	0.14		0.14

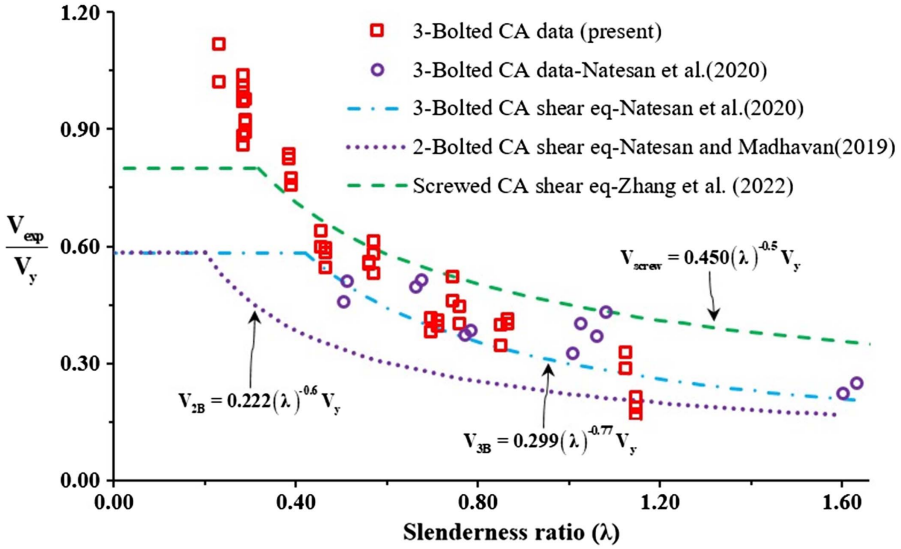

Fig. 21. Comparison of available shear equation with experimental data.

Table 9. Application of novel shear equation to the 2-bolt clip-angle

S. No.	Clip-angle configuration: *t-A-D*	Slenderness ratio (λ)	$\frac{p}{D}\lambda$	V_{exp} (kN)	Natesan and Madhavan (2019) eq. for 2-bolt CA: $V^1_{n2B} = 0.222(\lambda)^{-0.6})V_y$ (kN)	$\frac{V_{exp}}{V^1_{n2B}}$	Proposed equation for 2-bolt CA: $V_{n2B} = 0.12\,(\lambda p/D)^{-0.88}\,V_y$ (kN)	$\frac{V_{exp}}{V_{n2B}}$
1	1.5-65-100-2B	0.58	0.29	24.5	15.58	1.57	18.08	1.36
2	1.5-95-100-2B	1.12	0.56	17.16	10.46	1.64	10.08	1.70
3	1.5-125-100-2B	1.69	0.85	5.82	8.18	0.71	7.02	0.83

Table 9. (*Continued.*)

S. No.	Clip-angle configuration: *t-A-D*	Slenderness ratio (λ)	$\frac{p}{D}\lambda$	V_{exp} (kN)	Natesan and Madhavan (2019) eq. for 2-bolt CA: $V^1_{n2B} = 0.222(\lambda)^{-0.6})V_y$ (kN)	$\frac{V_{exp}}{V^1_{n2B}}$	Proposed equation for 2-bolt CA: $V_{n2B} = 0.12\ (\lambda p/D)^{-0.88}\ V_y$ (kN)	$\frac{V_{exp}}{V_{n2B}}$
4	1.5-65-150-2B	0.55	0.37	37.23	23.96	1.55	21.83	1.71
5	1.5-95-150-2B	1.08	0.72	24.27	16.09	1.51	12.17	1.99
6	1.5-125-150-2B	1.62	1.08	9.89	12.57	0.79	8.47	1.17
7	1.5-65-180-2B	0.54	0.39	34.26	29.07	1.18	24.81	1.38
8	1.5-95-180-2B	1.06	0.76	25.82	19.52	1.32	13.83	1.87
9	1.5-125-180-2B	1.59	1.15	16.19	15.25	1.06	9.63	1.68
10	2-65-100-2B	0.35	0.17	27.79	20.26	1.37	27.13	1.02
11	2-95-100-2B	0.68	0.34	16.68	13.46	1.24	14.89	1.12
12	2-125-100-2B	1.04	0.52	9.18	10.47	0.88	10.31	0.89
13	2-65-150-2B	0.33	0.22	40.83	31.14	1.31	32.75	1.25
14	2-95-150-2B	0.66	0.44	21.4	20.69	1.03	17.98	1.19
15	2-125-150-2B	1.00	0.66	15.63	16.10	0.97	12.45	1.26
16	2-65-180-2B	0.33	0.24	43.17	37.78	1.14	37.23	1.16
17	2-95-180-2B	0.64	0.47	32.48	25.10	1.29	20.44	1.59
18	2-125-180-2B	0.98	0.71	24.84	19.54	1.27	14.15	1.76
19	2.5-65-100-2B	0.26	0.13	31.96	27.85	1.15	40.24	0.79
20	2.5-95-100-2B	0.53	0.27	17.12	18.30	0.94	21.73	0.79
21	2.5-125-100-2B	0.81	0.41	11.32	14.18	0.80	14.95	0.76
22	2.5-65-150-2B	0.25	0.17	46.38	42.82	1.08	48.58	0.95
23	2.5-95-150-2B	0.51	0.34	32.12	28.13	1.14	26.23	1.22
24	2.5-125-150-2B	0.78	0.52	16.5	21.80	0.76	18.05	0.91
25	2.5-65-180-2B	0.25	0.18	48.16	51.95	0.93	55.21	0.87
26	2.5-95-180-2B	0.50	0.36	32.77	34.13	0.96	29.81	1.10
27	2.5-125-180-2B	0.77	0.55	28.32	26.45	1.07	20.52	1.38
For 2-bolt clip-angle configuration					Mean	1.14	From present Table 9 data	1.25
					Standard deviation	0.25		0.35
					Coefficient variation	0.22		0.28
For 3-bolt clip-angle configuration					Mean		From Table 8	1.06
					Standard deviation	—		0.15
					Coefficient variation			0.14
For 3-bolt and 2-bolt clip-angle configuration					Mean		From Tables 8 and 9 data	1.12
					Standard deviation	—		0.25
					Coefficient variation			0.22

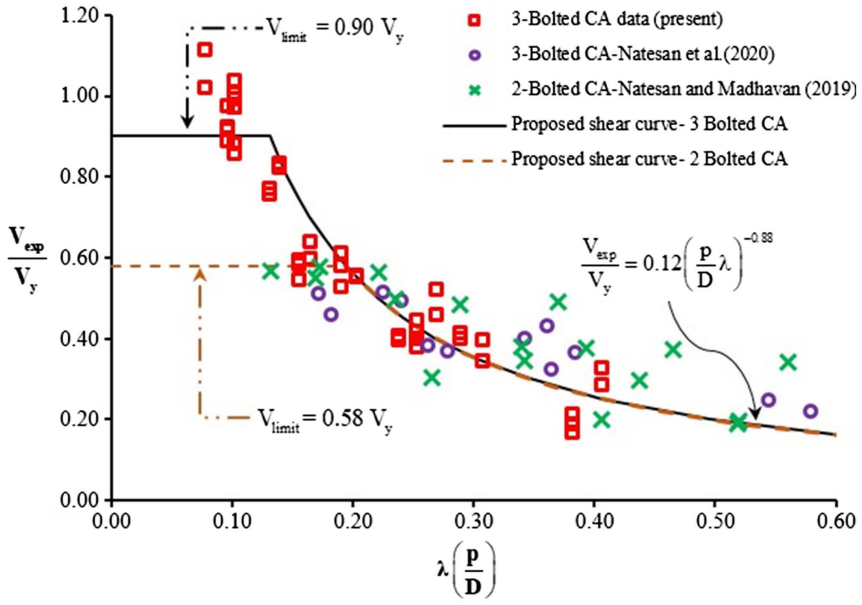

Fig. 22. New shear equation for the 2-bolt and 3-bolt configurations of clip-angle.

Table 10. Comparison of shear strength for 2-bolt and 3-bolt clip-angle

S. No.	Clip-angle configuration	Slenderness ratio (λ)	3-bolt CA: $V_{n3B} = 0.12(\lambda p/D)^{-0.88} V_y$ (kN)	2-bolt CA: $V^1_{n2B} = 0.222(\lambda)^{-0.6} V_y$ (kN)	% increase in shear strength $\frac{V_{n3B} - V^1_{n2B}}{V_{n2B}} \times 100$
1	1.5-65-150-3B-F1	0.391	25.90	14.26	82
2	1.5-65-150-3B-F2	0.391	25.90	14.26	82
3	1.5-95-150-3B-F1	0.760	14.44	9.58	51
4	1.5-95-150-3B-F2	0.760	14.44	9.58	51
5	1.5-125-150-3B-F1	1.147	10.05	7.48	34
6	1.5-125-150-3B-F2	1.147	10.05	7.48	34
7	1.5-65-180-3B-F1	0.384	31.58	17.30	83
8	1.5-65-180-3B-F2	0.384	31.58	17.30	83
9	1.5-95-180-3B-F1	0.746	17.61	11.62	52
10	1.5-95-180-3B-F2	0.746	17.61	11.62	52
11	1.5-125-180-3B-F1	1.126	12.26	9.08	35
12	1.5-125-180-3B-F2	1.126	12.26	9.08	35
13	2-65-150-3B-F1	0.289	47.45	24.00	98
14	2-65-150-3B-F2	0.289	47.45	24.00	98
15	2-95-150-3B-F1	0.571	26.04	15.94	63
16	2-95-150-3B-F2	0.571	26.04	15.94	63
17	2-125-150-3B-F1	0.867	18.03	12.41	45
18	2-125-150-3B-F2	0.867	18.03	12.41	45
19	2-65-180-3B-F1	0.283	57.87	29.12	99
20	2-65-180-3B-F2	0.283	57.87	29.12	99
21	2-95-180-3B-F1	0.560	31.76	19.34	64
22	2-95-180-3B-F2	0.560	31.76	19.34	64
23	2-125-180-3B-F1	0.851	21.99	15.05	46
24	2-125-180-3B-F2	0.851	21.99	15.05	46
25	2.5-95-150-3B-F1	0.465	41.98	24.27	73
26	2.5-95-150-3B-F2	0.465	41.98	24.27	73
27	2.5-125-150-3B-F1	0.712	28.89	18.81	54
28	2.5-125-150-3B-F2	0.712	28.89	18.81	54
29	2.5-95-180-3B-F1	0.457	51.19	29.44	74
30	2.5-95-180-3B-F2	0.457	51.19	29.44	74
31	2.5-125-180-3B-F1	0.699	35.23	22.82	54
32	2.5-125-180-3B-F2	0.699	35.23	22.82	54
33	1.5-125-150-3B-F3	1.147	10.05	7.48	34
34	2-95-150-3B-F3	0.571	26.04	15.94	63
35	2.5-95-150-3B-F3	0.465	41.98	24.27	73
36	2-65-150-3B-F1-HC	0.289	47.45	24.00	98
37	2-65-150-3B-F2-HC	0.289	47.45	24.00	98
38	2-65-180-3B-F1-HC	0.283	57.87	29.12	99
39	2-65-180-3B-F2-HC	0.283	57.87	29.12	99
40	2.5-65-150-3B-F1-HC	0.231	77.74	36.94	110
41	2.5-65-150-3B-F2-HC	0.231	77.74	36.94	110
42	2-65-180-3B-F3-HC	0.283	57.87	29.12	99
43	2-65-180-3B-F1-HC-10.9	0.283	57.87	29.12	99
44	2-65-180-3B-F2-HC-10.9	0.283	57.87	29.12	99
45	2.5-65-150-3B-F1-HC-10.9	0.231	90.15	44.45	103
46	2.5-65-150-3B-F2-HC-10.9	0.231	90.15	44.45	103
47	2.5-65-180-3B-F1-HC-10.9	0.227	109.95	53.94	104
48	2.5-65-180-3B-F2-HC-10.9	0.227	109.95	53.94	104

is relatively higher for clip-angles with a lower slenderness ratio (<0.80), while it is relatively lower for those with a higher slenderness ratio, as shown in Fig. 23 and Table 10.

Reliability Study of the 3-Bolt and 2-Bolt Clip-Angles

Reliability analysis was performed for the suggested shear strength equation and the shear equation previously proposed by Natesan et al. (2020), as provided in Table 11. Resistance and safety factors were calculated for fixed target reliability index values according to the load and resistance factor design (LRFD), limit state design (LSD), and allowable strength design (ASD) design methods. The target reliability value (ϕ) was calculated by

$$\phi = C_\phi \times M_m \times F_m \times P_m \times e^{-\beta_0 \sqrt{V_M^2 + V_F^2 + C_P V_P^2 + V_Q^2}} \quad (4)$$

where C_Φ = calibration coefficient = 1.52 for the LRFD method and = 1.42 for the LSD method; M_m = mean of the material factor; F_m = mean of the fabrication factor; P_m = mean of the professional factor; β_0 = target reliability index value = 3.5 for connections for the LRFD method and = 4 for connections for the LSD method;

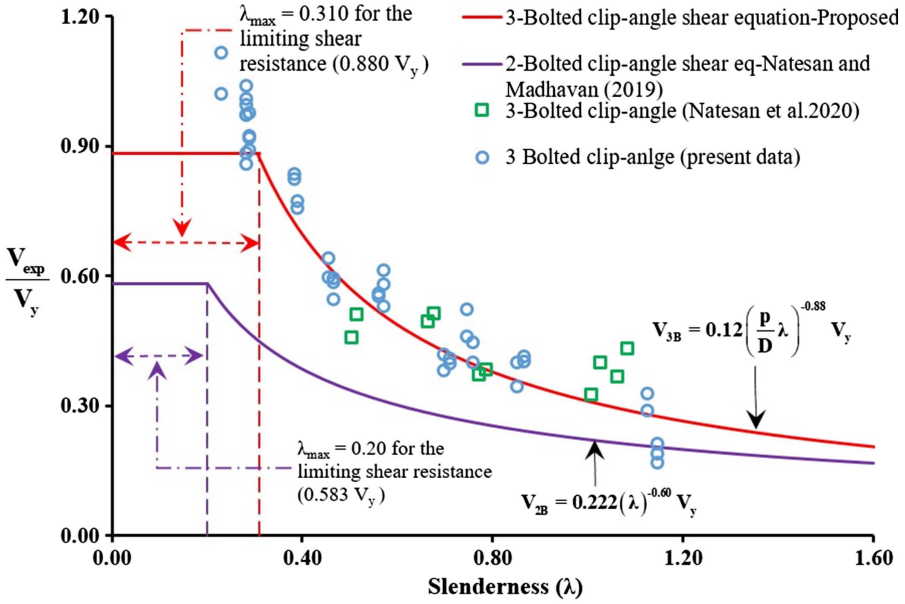

Fig. 23. Shear strength comparison of 2-bolt and 3-bolt configuration of clip-angle.

Table 11. Reliability analysis of shear strength equations

Description	3-bolt shear equation by Natesan et al. (2020) [from Eq. (1)]	Proposed eq. for 3-bolt CA [from Eq. (2)]	Proposed eq. for 2-bolt CA [from Eq. (2)]	For bolted (3-bolt, 2-bolt) CA [from Eq. (2)]
No. of tests conducted (n)	60	60	27	87
Degrees of freedom (m)	59	59	26	86
Mean value of professional factor (P_M)	1.16	1.06	1.25	1.12
Standard deviation (σ)	0.16	0.15	0.35	0.25
Coefficient of variation of test results (V_p)	0.14	0.14	0.28	0.22
Correction factor (C_p)	1.05	1.05	1.12	1.04
Mean value of material factor (M_M)	1.1	1.1	1.1	1.1
Mean value of fabrication factor (F_M)	1	1	1	1
Calibration coefficient (C_Φ): LRFD	1.52	1.52	1.52	1.52
Calibration coefficient (C_Φ): LSD	1.42	1.42	1.42	1.42
Coefficient of variation of material factor (V_M)	0.08	0.08	0.08	0.08
Coefficient of variation of fabrication factor (V_F)	0.15	0.15	0.15	0.15
Coefficient of variation of load effects (V_Q)	0.21	0.21	0.21	0.21
Target reliability index (β_o): LRFD	3.5	3.5	3.5	3.5
Target reliability index (β_o): LSD	4	4	4	4
Resistance factor (Φ): LRFD	0.66	0.61	0.51	0.55
Resistance factor (Φ): LSD	0.53	0.49	0.39	0.43
Safety factor: ASD	2.41	2.63	3.12	2.92

V_M = coefficient of variation of the material factor; V_F = coefficient of variation of fabrication factor; C_P = correction factor = $[1 + (1/n)] \times [m/(m-2)]$ if $n \geq 4$; n = number of tests conducted; $m = n - 1$ = degrees of freedom; V_P = coefficient of variation of experimental results ≤6.5; V_Q = coefficient of variation of load effects = 0.21 for LRFD and LSD methods; and Ω = safety factor = $1.6/\phi_{LRFD}$.

The proposed new shear strength equation [Eq. (2)] for a 3-bolt clip-angle yields lesser resistance factor values (0.61 and 0.49) for the LRFD and LSD methods than the Natesan et al. (2020) suggested shear equation (0.66 and 0.53). These smaller resistance factors reflect the more serious nature of the clip-angle failure that results in fracture of the clip-angle. In the present study, a similar result occurred, as the clip-angle was subjected to tearing failure. A higher safety factor (2.63) was obtained for the suggested new shear equation than for the Natesan et al. (2020) shear equation (2.41) for a 3-bolt clip-angle configuration. From the proposed design shear equation [Eq. (2)] the design factors of 0.51, 0.39, and 3.12 were suggested for the 2-bolt clip-angle configuration for the LRFD, LSD, and ASD methods, respectively (refer to Table 11). From the collated data of 2-bolt (Natesan and Madhavan 2019) and 3-bolt (present study and Natesan et al. 2020) configurations, the design factors of 0.55, 0.43, and 2.92 were recommended for the bolted configuration of the CFS clip-angle connection.

Conclusions

- An optimized ultimate shear strength equation for the three bolt clip-angle was proposed after calibration against 54 laboratory tests.

- The three bolt clip-angles with aspect ratios $(L/D) \leq 0.23$ will be subjected to tearing failure while the clip-angles with $(L/D) > 0.23$ fail due to shear local buckling.
- The comparative study of two bolt and three bolt clip-angles indicates that the addition of a bolt increases the strength of the clip-angle significantly. This increase is relatively higher for slenderness ratios <0.8 than for those ≥ 0.8.
- From the reliability analysis, design factors of 0.55, 0.43, and 2.92 were suggested for the LRFD, LSD, and ASD methods for design strength calculation of a bolted clip-angle configuration using 2-bolt and 3-bolt configuration data.

Appendix I. Design Example

Find the increase in shear strength of a 2-bolt clip-angle, for the addition of a bolt in the same bolt line. Geometric details of the clip-angles are illustrated in Fig. 24. and other details are as follows:

Corner radius, $R = 3$ mm
Yield strength, $f_y = 350$ MPa
Young's modulus, $E = 2 \times 10^5$ MPa
Poisson's ratio, $\mu = 0.3$

Appendix II. Slenderness Ratio of the Clip-Angle

Flat width of out-standing leg, $L = 80 - 2 - 3 = 75$ mm

Aspect ratio of clip-angle out-standing leg, $L/D = 75/180 = 0.416 > 0.23$

As $(L/D) > 0.23$, clip-angle will be subjected to shear local buckling

Elastic buckling coefficient, $k = 2.569(\frac{L}{D})^{-2.202} = 17.72$

Critical buckling stress $f_{cr} = \frac{k\pi^2 E}{12(1-\mu^2)}(\frac{t}{D})^2 = 395.44$ N/mm^2
Critical shear strength, $V_{cr} = f_{cr} \times t \times D = 142.36$ kN
Yield shear strength, $V_y = 0.6 f_y \times t \times D = 75.60$ kN

Slenderness ratio, $\lambda = \sqrt{\frac{75.60}{142.26}} = 0.729$

Appendix III. Design Shear Strength Calculation

Pitch ratio = $\frac{p}{D} = \frac{60}{180} = 0.33$

For 3-bolt configuration: $\lambda(\frac{p}{D})_{3B} = 0.729 \times 0.33 = 0.243$

Nominal shear strength of 3-bolt clip-angle from the proposed new shear strength Eq. (2)

$$V_{n-3B} = 0.12\left(\frac{p}{D}\lambda\right)_{3B}^{-0.88} \tag{5}$$

$$V_{n-3B} = 0.12 \times (0.243)^{-0.88} \times 75.60 = 31.50 \text{ kN}$$

Design shear strength values calculated as
For LRFD method:

$$V_{d-\text{LRFD}} = \phi_{\text{LRFD}} \times V_{n3B} = 0.61 \times 31.50 = 19.21 \text{ kN}$$

For LSD method:

$$V_{d-LSD} = \phi_{LSD} \times V_{n3B} = 0.49 \times 31.50 = 15.43 \text{ kN}$$

For ASD method:

$$V_{d-\text{ASD}} = \frac{V_{n-3B}}{\Omega_{\text{ASD}}} = \frac{31.50}{2.63} = 11.98 \text{ kN}$$

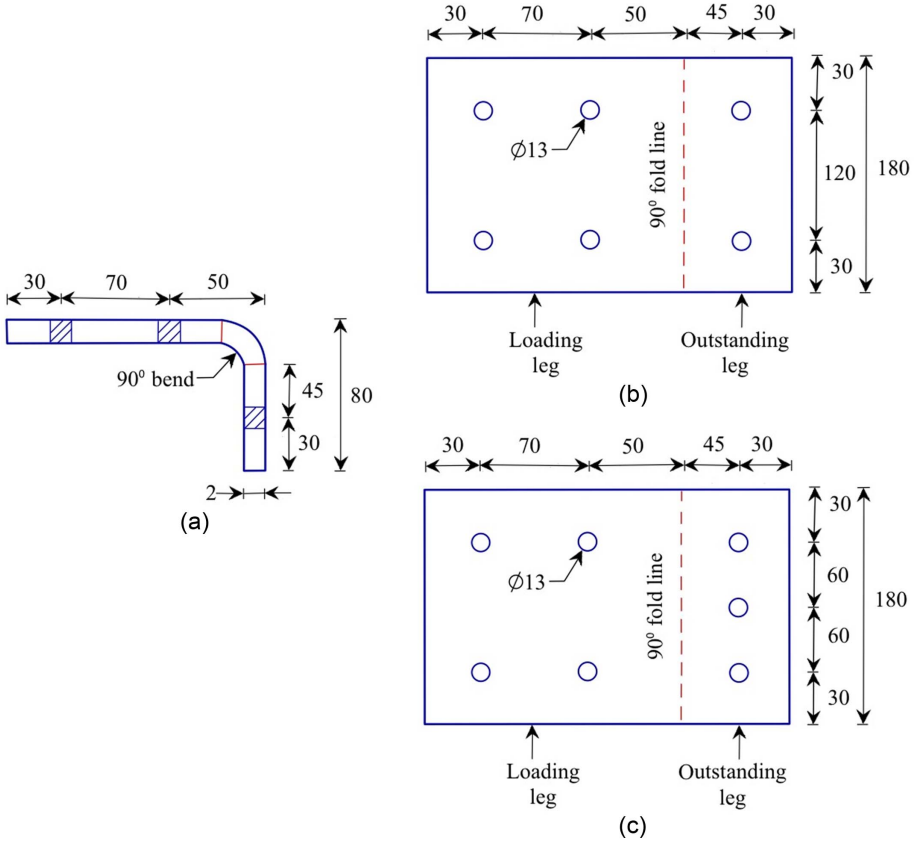

Fig. 24. (a) Top view; (b) flat view of 2-bolt clip-angle; and (c) flat view of 3-bolt clip-angle.

J. Struct. Eng., 2023, 149(5): 04023048

Appendix IV. Shear Strength Comparison of 2-Bolt and 3-Bolt Configurations

Pitch ratio = $\frac{p}{D} = \frac{120}{180} = 0.66$

For 2-bolt configuration: $\lambda(\frac{p}{D})_{2B} = 0.729 \times 0.66 = 0.481$

Nominal shear strength of 2-bolt clip-angle from the proposed shear equation [Eq. (4)]

$$V_{n-2B} = 0.12\left(\frac{p}{D}\lambda\right)_{2B}^{-0.88}$$

$$V_{n-3B} = 0.12 \times (0.481)^{-0.88} \times 75.60 = 17.27 \text{ kN}$$

Design shear strength values calculated as

For LRFD method:

$$V_{d-\text{LRFD}} = \phi_{\text{LRFD}} \times V_{n-2B} = 0.51 \times 17.27 = 8.80 \text{ kN}$$

For LSD method:

$$V_{d-\text{LSD}} = \phi_{\text{LSD}} \times V_{n-2B} = 0.39 \times 17.27 = 6.73 \text{ kN}$$

For ASD method:

$$V_{d-\text{ASD}} = \frac{V_{n-2B}}{\Omega_{\text{ASD}}} = \frac{17.27}{3.12} = 5.53 \text{ kN}$$

Percent increase in shear strength of clip-angle for 3-bolt configuration over 2-bolt configuration

$$= \frac{V_{n-3B} - V_{n-2B}}{V_{n-2B}} \times 100$$

$$= \frac{31.50 - 17.27}{17.27} \times 100$$

$$= 5.53 \text{ kN}$$

Hence, with the addition of a bolt to a 2-bolt configured clip-angles, ultimate shear strength increases by 82.4%.

Data Availability Statement

Some or all data used during the study are available from the corresponding author by request, including the values used for plotting the figures, the design calculation procedure and photographs of failure modes of test specimens.

Acknowledgments

The authors would like to thank the Ministry of Education (MoE) of India for the financial support in the form of a fellowship for this research.

Notation

The following symbols are used in this paper:

A = width of out-standing leg of clip-angle;
C_Φ = calibration coefficient;
D = depth of clip-angle;
E = young's modulus of steel;
F_m = mean of fabrication factor;
f_{cr} = elastic critical buckling stress;
f_y = steel yield strength;
f_u = steel ultimate strength;
k = buckling coefficient;
L = flat width of out-standing leg of clip-angle;
L/D = aspect ratio of clip-angle;
M_m = mean of material factor;
P_m = mean of professional factor;
V_F = coefficient of variation for fabrication factor;
V_M = coefficient of variation for material factor;
V_P = coefficient of variation for experimental results;
V_Q = coefficient of variation for load effects;
V_{cr} = critical shear strength;
V_d = design shear strength;
V_{n2B} = nominal shear capacity of clip-angle with 2 bolts configuration;
V_{n3B} = nominal shear capacity of clip-angle with 3 bolts configuration;
V_y = yield strength in shear;
Ω = safety factor (ASD);
β = target reliability index value;
λ = non-dimensional slenderness ratio;
μ = steel Poisson's ratio; and
Φ = resistance factor (LRFD, LSD).

References

AISI (American Iron and Steel Institute). 2016. *North American specification for the design of cold-formed steel structural members*. AISI S100-16. Washington, DC: AISI.

ASTM. 2010. *Standard test methods for tension testing of metallic materials*. ASTM E8/E8M. West Conshohocken, PA: ASTM.

Fox, S. R. 2005. *Strength of CFS floor assemblies with clip angle bearing stiffeners*. AISI research report. Washington, DC: AISI.

Huang, Y., and B. Young. 2014. "The art of coupon tests." *J. Constr. Steel Res.* 96 (May): 159–175. https://doi.org/10.1016/j.jcsr.2014.01.010.

Natesan, V., and M. Madhavan. 2019. "Experimental study on beam-to-column clip angle bolted connection." *Thin-Walled Struct.* 141 (Aug): 540–553. https://doi.org/10.1016/j.tws.2019.04.048.

Natesan, V., B. Shanmugasundaram, and M. Madhavan. 2020. "Comparative experimental studies on the web cleat bolted CFS beam-to-column connection." *J. Constr. Steel Res.* 170 (Jul): 106080. https://doi.org/10.1016/j.jcsr.2020.106080.

Natesan, V., B. Shanmugasundaram, M. Sekar, and M. Madhavan. 2021. "Effectiveness of CFS web cleat bolted connections between beam–to–column." *Structures* 33 (Oct): 3269–3283. https://doi.org/10.1016/j.istruc.2021.06.067.

Obeydi, M., M. Daei, M. Zeynalian, and M. Abbasi. 2021. "Numerical modeling on thin-walled cold-formed steel clip angles subjected to pull-out failures." *Thin-Walled Struct.* 164 (Jul): 107716. https://doi.org/10.1016/j.tws.2021.107716.

Obeydi, M., M. Zeynalian, and M. Daei. 2020. "An experimental study of screw pull-out in load bearing cold-formed-steel clip angles." *J. Constr. Steel Res.* 166 (Mar): 105931. https://doi.org/10.1016/j.jcsr.2020.105931.

Redwood, R. G., and D. G. Eyre. 1984. "Clip angle connections subjected to cyclic loads." *J. Struct. Eng.* 110 (1): 162–166. https://doi.org/10.1061/(ASCE)0733-9445(1984)110:1(162).

Yam, M. C. H., Y. C. Zhong, A. C. C. Lam, and V. P. Iu. 2007a. "An investigation of the block shear strength of coped beams with a welded clip angle connection—Part I: Experimental study." *J. Constr. Steel Res.* 63 (1): 96–134. https://doi.org/10.1016/j.jcsr.2006.03.011.

Yam, M. C. H., Y. C. Zhong, A. C. C. Lam, and V. P. Iu. 2007b. "An investigation of the block shear strength of coped beams with a welded clip angle connection—Part II: Numerical study." *J. Constr. Steel Res.* 63 (1): 116–134. https://doi.org/10.1016/j.jcsr.2006.03.010.

Yu, C., Z. Yan, W. Zhang, and L. Qian. 2018. *Load bearing clip angle design—Phase II*. Rep. No. RP18—4. Washington, DC: American Iron and Steel Institute.

Yu, C., M. Yousof, and M. Mahdavian. 2015. *Load bearing clip angle design*. Rep. No. UNT-GP6351. Washington, DC: American Iron and Steel Institute.

Yu, C., M. Yousof, M. Mahdavian, and W. Z. Mahdavian. 2016. "Behavior and design of thin-walled cold-formed steel clip angles subjected to shear load." *J. Struct. Eng.* 142 (7): 04016040. https://doi.org/10.1061/(ASCE)ST.1943-541X.0001493.

Yu, C., M. Yousof, M. Mahdavian, and W. Zhang. 2017. "Design of cold-formed steel clip angles in compression." *J. Struct. Eng.* 143 (6): 04017030. https://doi.org/10.1061/(ASCE)ST.1943-541X.0001767.

Zhang, W., Y. Liu, X. Xu, and C. Yu. 2022. "Improved shear design method of cold-formed steel clip angles." *J. Constr. Steel Res.* 188 (Jan): 107045. https://doi.org/10.1016/j.jcsr.2021.107045.

Zhang, W., M. Mahdavian, M. Yousof, and Y. Cheng. 2018. "Testing and design of cold-formed steel clip angles in tension: Pull-over and serviceability." *Thin-Walled Struct.* 124 (Mar): 13–19. https://doi.org/10.1016/j.tws.2017.11.049.